Journal Pre-proof

Synthesis, biological and molecular dynamics investigations with a series of triazolopyrimidine/triazole-based benzenesulfonamides as novel carbonic anhydrase inhibitors

Mohamed A. Said, Wagdy M. Eldehna, Alessio Nocentini, Alessandro Bonardi, Samar H. Fahim, Silvia Bua, Dalia H. Soliman, Hatem A. Abdel-Aziz, Paola Gratteri, Sahar M. Abou-Seri, Claudiu T. Supuran

PII: S0223-5234(19)30995-X

DOI: https://doi.org/10.1016/j.ejmech.2019.111843

Reference: EJMECH 111843

To appear in: *European Journal of Medicinal Chemistry*

Received Date: 15 October 2019

Revised Date: 31 October 2019

Accepted Date: 31 October 2019

Please cite this article as: M.A. Said, W.M. Eldehna, A. Nocentini, A. Bonardi, S.H. Fahim, S. Bua, D.H. Soliman, H.A. Abdel-Aziz, P. Gratteri, S.M. Abou-Seri, C.T. Supuran, Synthesis, biological and molecular dynamics investigations with a series of triazolopyrimidine/triazole-based benzenesulfonamides as novel carbonic anhydrase inhibitors, *European Journal of Medicinal Chemistry* (2019), doi: https://doi.org/10.1016/j.ejmech.2019.111843.

Graphical Abstract

Synthesis, biological and molecular dynamics investigations with a series of triazolopyrimidine/triazole-based benzenesulfonamides as novel carbonic anhydrase inhibitors

New sets of triazolopyrimidine-based (**9a-d**) and triazole-based (**11a-h**, **13a-c**, **15a**,**b**, **17a**,**b** and **21a-g**) benzenesulfonamides were synthesized and evaluated for their inhibitory activity toward a panel of carbonic anhydrase isoforms hCA I, II, IX and XII. hCA IX and XII isoforms were efficiently inhibited with K_Is range of 3.3-85 nM and 4.4-105 nM. Compounds **9d** and **21e** were found to be the most selective *h*CA IX inhibitors over *h*CA I and *h*CA II.

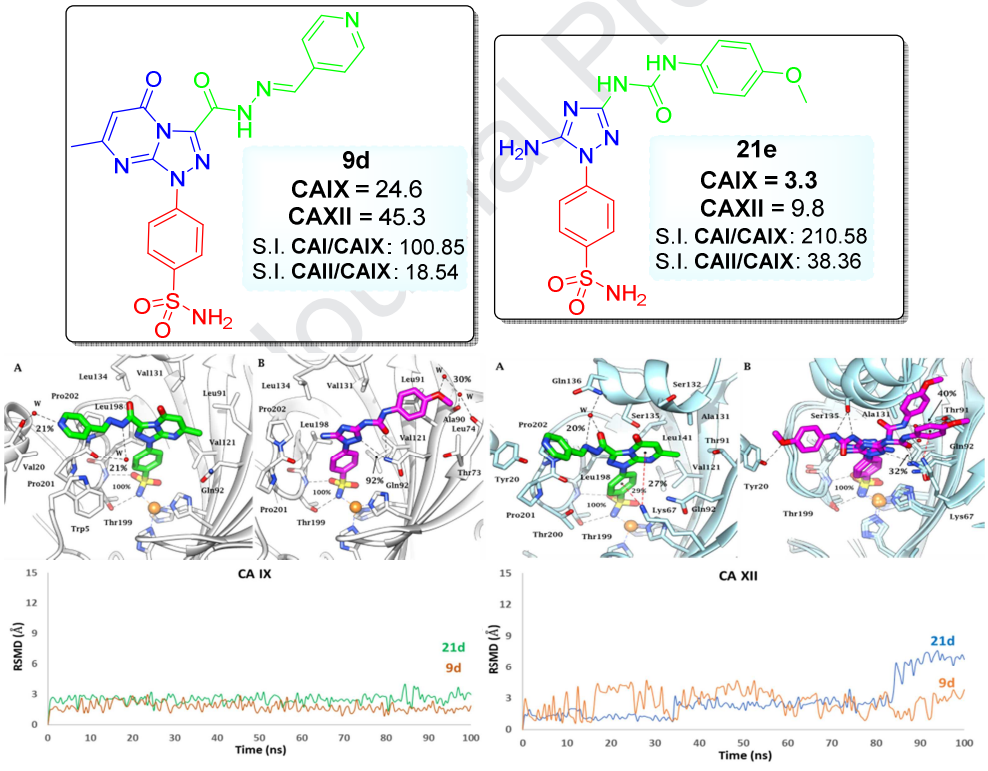

Synthesis, biological and molecular dynamics investigations with a series of triazolopyrimidine/triazole-based benzenesulfonamides as novel carbonic anhydrase inhibitors

Mohamed A. Said[a], Wagdy M. Eldehna[b,*], Alessio Nocentini[c,d], Alessandro Bonardi[c,d], Samar H. Fahim[e], Silvia Bua[c], Dalia H. Soliman[a,f], Hatem A. Abdel-Aziz[g], Paola Gratteri[d], Sahar M. Abou-Seri[e], Claudiu T. Supuran[c,*]

[a] *Department of Pharmaceutical Chemistry, College of Pharmacy, Egyptian Russian University, Badr City, Cairo, P.O. Box 11829, Egypt*
[b] *Department of Pharmaceutical Chemistry, Faculty of Pharmacy, Kafrelsheikh University, Kafrelsheikh, P.O. Box 33516, Egypt*
[c] *Department of NEUROFARBA, Section of Pharmaceutical and Nutraceutical Sciences, University of Florence, Polo Scientifico, Via U. Schiff 6, 50019, Sesto Fiorentino, Firenze, Italy*
[d] *Department of NEUROFARBA – Pharmaceutical and nutraceutical section; Laboratory of Molecular Modeling Cheminformatics & QSAR, University of Firenze, Via U. Schiff 6, 50019 Sesto Fiorentino, Firenze, Italy*
[e] *Department of Pharmaceutical Chemistry, Faculty of Pharmacy, Cairo University, Kasr El-Aini Street, Cairo, P.O. Box 11562, Egypt*
[f] *Department of Pharmaceutical Chemistry, Faculty of Pharmacy, Al Azhar University, Cairo, P.O. Box 11471, Egypt*
[g] *Department of Applied Organic Chemistry, National Research Center, Dokki, Cairo 12622, Egypt*

ABSTRACT

In the presented work, we report the design and synthesis of different new sets of triazolopyrimidine-based (**9a-d**) and triazole-based (**11a-h**, **13a-c**, **15a**,**b**, **17a**,**b** and **21a-g**) benzenesulfonamides. The newly synthesized sulfonamides were assessed for their inhibitory activities toward four human (*h*) metalloenzyme carbonic anhydrase (CA, EC 4.2.1.1) isoforms; *h*CA I, II, IX and XII. The four examined isoforms were inhibited by the prepared sulfonamides (**9a-d**, **11a-h**, **13a-c**, **15a**,**b**, **17a**,**b** and **21a-g**) in variable degrees with K_Is ranges: 94.4-4953.5 nM for hCA I, 6.9-837.6 nM for hCA II, 3.3-85.0 nM for hCA XI, and 4.4-105.0 nM for hCA XII. In particular, sulfonamides **11e, 21a** and **21e** emerged as single-digit nanomolar hCA IX and hCA XII inhibitors. Interestingly, triazolopyrimidine-based sulfonamide **9d** and triazole-based sulfonamide **21e** were found to be the most selective *h*CA IX inhibitors over *h*CA I (SI = 100.85 and 210.58, respectively) and *h*CA II (SI = 18.54 and 38.36, respectively). Thereafter,

sulfonamides **9d** and **21e** were docked into the active site of CAs II, IX and XII, then poses showing the best scoring values and favorable binding interactions were subjected to a MM-GBSA based refinement and, limited to CA IX and XII, to a cycle of 100 ns molecular dynamics.

_____

Keywords: Carbonic anhydrase inhibitors; Molecular dynamics; Triazoles; Triazolopyrimidines; Synthesis.

* Corresponding authors. E-mail addresses: wagdy2000@gmail.com (W.M. Eldehna), claudiu.supuran@unifi.it (C.T. Supuran).

1. Introduction

The α-class carbonic anhydrases (CA) are a family of zinc-containing metallo-enzymes that is composed of sixteen isoforms which differ in tissue expression patterns, function and kinetic properties.[1, 2] The sluggishness and overexpression of various CA isoforms are responsible for many diseases in human beings.[1] Involvement of CA I and CA II in many important normal physiological processes such as regulation of the acid–base homeostasis made them act as worthy drug targets in glaucoma, cerebral edema and epilepsy.[3] On the other hand, the expression of CA IX and CA XII is limited in normal tissues, but their induction by the hypoxic conditions in several cancer cell lines made them valuable targets as anticancer agents. CA IX and CA XII have a role in the conversion of CO_2 to HCO_3^- and a proton, then facilitating the diffusion of that proton through the entire solid tumor leading to low extracellular pH that expedite matrix breakdown, invasion, and multi-drug resistance.[1, 4] hCA IX isoform is highly observed in many aggressive tumors including breast, ovarian, bladder, cervix, colorectal, kidney, lung, pancreatic, head and neck, stomach and oral cavity cancers.[5] Whereas, hCA XII isoform was robustly expressed in glioblastomas, lung carcinomas, breast carcinoma, urinary bladder cell carcinomas and T-cell lymphomas.[5]

The design of compounds exhibiting both great affinity and high CA isoform-selectivity for the specific disease treatment without causing side effects due to off-target CA modulation is a challenging task because of the high structural homology among human CAs, especially within their active sites.[6] The CA active site is located in cone-shaped cavity (approximately 15Å deep). The catalytic zinc ion is situated near the bottom of the cavity and is coordinated to the side chains of three conserved histidine residues and a water molecule/hydroxide ion. The cavity extends to the center of the molecule with hydrophobic residues forming one side of the cavity and hydrophilic residues for the other side. Although, the core of active site is highly conserved among human CAs, residues of its periphery (10 Å –15 Å from the zinc) are variable in terms of the polarity and hydrophobicity.[7] This part of the active site is defined as the selectivity pocket and is used to design ligands targeting the specific CA isoform.

The most successful strategies of modulating CA IX/XII catalytic activities to date include the application of sulfonamide function as zinc anchoring group, however only few

sulfonamide derivatives have progressed to clinical trials due to lack of selectivity. Among the different approaches used for development of isoform selective carbonic anhydrase inhibitors (CAIs) the tail approach is most widely employed. In the tail approach, the aromatic sulfonamide ring, zinc anchoring group, is appended with tail moieties through flexible functionalized linkers. The tails and linkers are selected to modulate interactions with amino acid residues from the middle and edge of the enzyme active site seeking for isoform-selective inhibition profiles and /or enhancing the physicochemical properties of the molecule. A flexible hydrophobic tail group will generally adopt a conformation to interact with the hydrophobic half of the CA active site; similarly, a flexible hydrophilic tail substituent will generally interact with the hydrophilic half of the CA active site. A successful example for this approach is the novel CA IX inhibitor SLC-0111 **I** (**Fig.** 1). This novel drug is now in Phase 1b/II clinical trials for the treatment of advanced and metastatic solid tumors [8]

Literature survey regarding several human carbonic anhydrase inhibitors revealed that, triazole and fused triazole-linked benzenesulfonamides (as compounds **II-VI**) have been emerged as important classes of potent CAIs with much higher selectivity towards the tumor-associated isoforms; CA IX and XII than on the ubiquitously expressed isoforms CA I and II (**Fig.** 1). [9-12] Furthermore, the triazolo moiety enhanced hydro-solubility of the target molecules such as compound **IV** (**Fig. 1**).[11] While fused triazoles revealed better hydrophilic/hydrophobic ratio so as to improve solubility and CA receptor fitting in both hydrophilic and hydrophobic pockets as seen in compounds **V** and **VI** .[10, 12].

In continuation to our previous work in the search for potent and selective hCA IX and hCA XII inhibitors [13-16], we report herein the design and synthesis of new sets of triazolopyrimidine- and triazole-based benzenesulfonamides (**9a-d, 11a-h, 13a-c**, **15a,b**, **17a,b** and **21a-g**), as potential CA IX and hCA XII inhibitors. The design of the new compounds relies on applying the tail approach. The triazole/triazolopyrimidine benzenesulfonamide scaffold was connected to an aryl tail through different functionalized linker as hydrazide-hydrazone (**9a-d**, **11a-h** and **13a-c**), semicarbazide/thiosemicarbazide (**15a,b** and **17a,b**) or ureido (**21a-g**). Such linkers are selected to donate different levels of flexibility to the aryl tail and impart the possibility for the new compounds to adopt a diversity of orientations that may permit the specific interactions between the tail and amino acid residues at the entrance of carbonic

anhydrase active site (selectivity pocket). Furthermore, the aryl was designed to ensure different electronic, hydrophilic and lipophilic environments to explore a valuable SAR.

The newly synthesized sulfonamides were assessed for their inhibitory activities against four CA isoforms (hCA I, hCA II, hCA IX and hCA XII). In addition, sulfonamides **9d** and **21e** were docked into the active site of CAs II, IX and XII, then poses showing the best scoring values and favorable binding interactions were subjected to a MM-GBSA based refinement and, limited to CA IX and XII, to a cycle of 100 ns molecular dynamics.

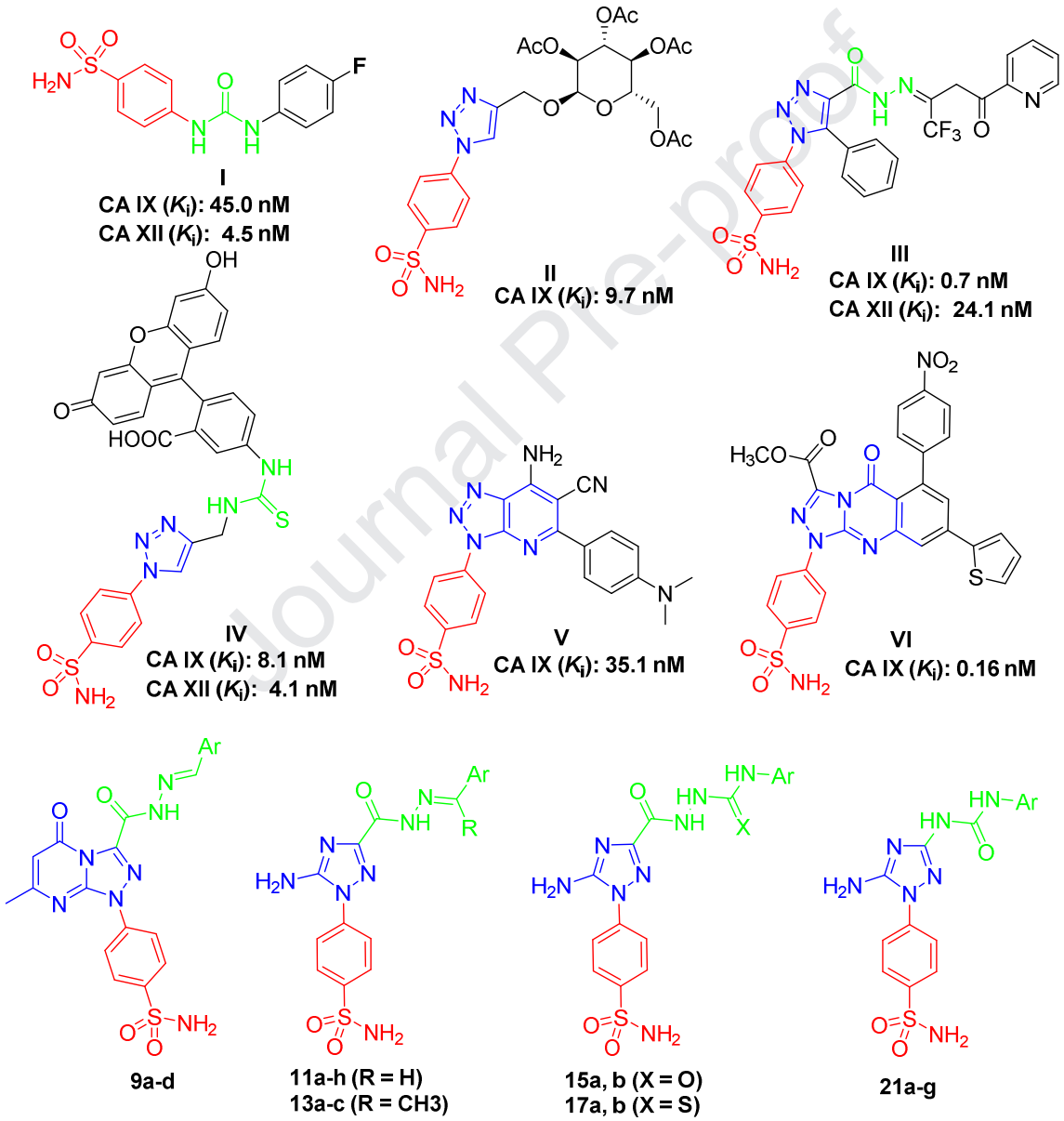

Fig. 1. Structures of certain triazolopyrimidine/triazole-based CAIs **I-VI**, and structures of the target sulfonamides **9a-d, 11a-h, 13a-c**, **15a,b**, **17a,b** and **21a-g**

2. Results and Discussion

2.1. Chemistry

The synthetic pathways employed to prepare the key intermediates and the new targeted derivatives are depicted in **Schemes 1-4**. Synthesis of 6-methyl-2-thiouracil **2** was achieved by refluxing ethyl acetoacetate **1** and thiourea in sodium ethoxide through hetero-cyclocondensation reaction.[17] Subsequently, preparation of the key intermediate ethyl [1,2,4]triazolo[4,3-*a*]pyrimidine-3-carboxylate **5** was carried out through refluxing 6-methyl-2-thiouracil **2** with the hydrazonoyl chloride **3** in dioxane in the presence of a catalytic amount of triethylamine with 41% yield. The reaction mechanism proceeds through S-alkylation reaction to give intermediate **4** followed by the Smiles rearrangement (**Scheme 1**).[18] ^{1}H NMR spectrum of **5** showed a D_2O-exchangeable singlet signal attributable to the (NH_2) protons of sulfonamido group at δ 7.47 *ppm*, whereas the unique H-6 triazolopyrimidine proton appeared as a singlet signal at δ 6.02 *ppm*, in addition to the singlet corresponding to the 7-methyl triazolopyrimidine protons which resonated at δ 2.34 *ppm*. Finally, the terminal ethyl group of the ester moiety appeared as a triplet signal for methyl protons at δ 1.32 *ppm* and a quartet signal for CH_2 protons at δ 4.45 *ppm*.

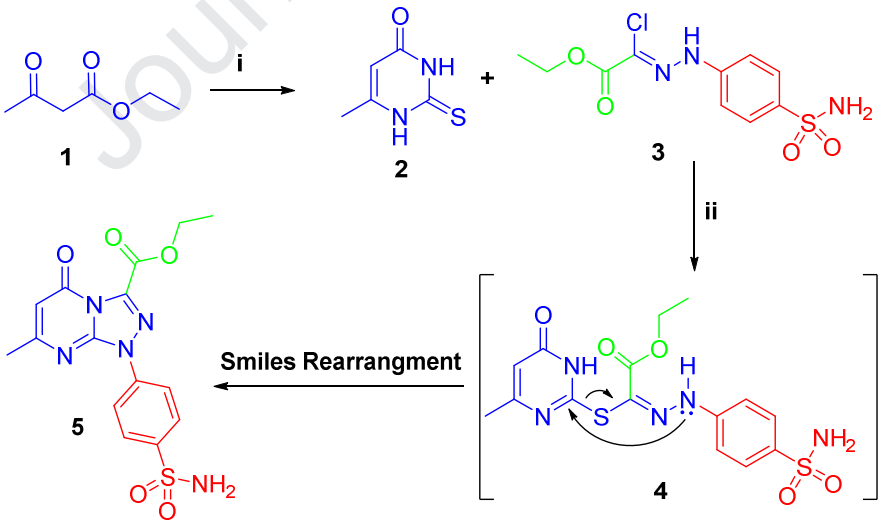

Scheme 1. *Reagents and conditions*: **i.** Thiourea, NaOEt, reflux, 7h; **ii.** Dioxan, TEA, reflux 12h.

Interestingly, hydrazinolysis of the ester derivative **5** yielded two different hydrazide products (**6** and **7**) depending on the molar ratio of hydrazine hydrate and the reaction time.

Applying two equivalents of hydrazine hydrate in refluxing ethanol for two hours afforded the expected fused triazolo[4,3-*a*]pyrimidine hydrazide **6**, whereas, refluxing ester **5** with ten equivalents of hydrazine hydrate for eight hours resulted in hydrazinolysis of not only the ester group, but also the triazolopyrimidine ring affording the monocyclic 4-(5-amino-3-(hydrazinecarbonyl)-*1H*-1,2,4-triazol-1-yl)benzenesulfonamide **7**. The former bicyclic hydrazide **6** was heated with different aldehydes in ethanol in the presence of catalytic amount of glacial acetic acid to afford target compounds **9a-d** (**Scheme 2**).[19] ^{1}H NMR spectrum of **6** revealed the presence of three D_2O exchangeable singlet signals assigned to the NH_2 and NH groups of the hydrazide function at δ 4.87 and 10.52 *ppm* as well as the sulfonamide NH_2 at 7.52 *ppm*. Also, the spectrum showed two singlets at δ 2.39 and 6.09 *ppm* corresponding to the methyl protons and the H-6 triazolopyrimidine proton, respectively. On the other hand, ^{1}H NMR spectrum of hydrazide **7** revealed the absence of C-7 methyl protons and C-6 proton of the triazolopyrimidine nucleus, concurrently with the appearance of new D_2O exchangeable singlet signal at δ 6.82 *ppm* attributable for NH_2 group at position 5 of the triazole ring, in addition to the presence of the D_2O exchangeable protons of the hydrazide function (CONHNH$_2$) and sulfonamido (SO_2NH_2) group at δ 4.51, 9.44 and 7.51 *ppm*, respectively. Moreover, the HRMS data supported the structure of hydrazide **7** by a molecular ion peak at *m/z* 298.07171.

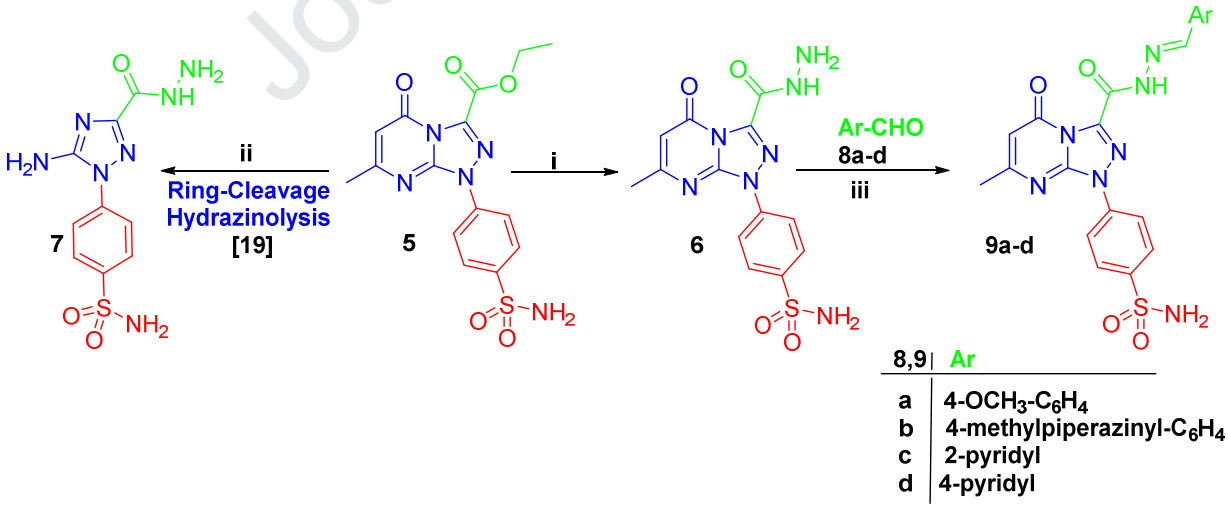

Scheme 2. Reagents and conditions: i. $NH_2NH_2.H_2O$ (2 eq.), EtOH, reflux 2h; **ii.** Xss $NH_2NH_2.H_2O$ (10 eq.), EtOH, reflux 8h; **iii.** EtOH, AcOH, reflux 2h.

In **Scheme 3**, hydrazide **7** was reacted with different aromatic aldehydes **10a-h** and acetophenones **12a-c** in glacial acetic acid to furnish the target sulfonamides **11a-h** or **13a-c**, respectively. Alternatively, refluxing the key intermediate **7** with aryl isocyanates **14a,b** or aryl isothiocynates **16a,b** in dry toluene afforded the target sulfonamides **15a,b** and **17a,b**, respectively (**Scheme 3**).

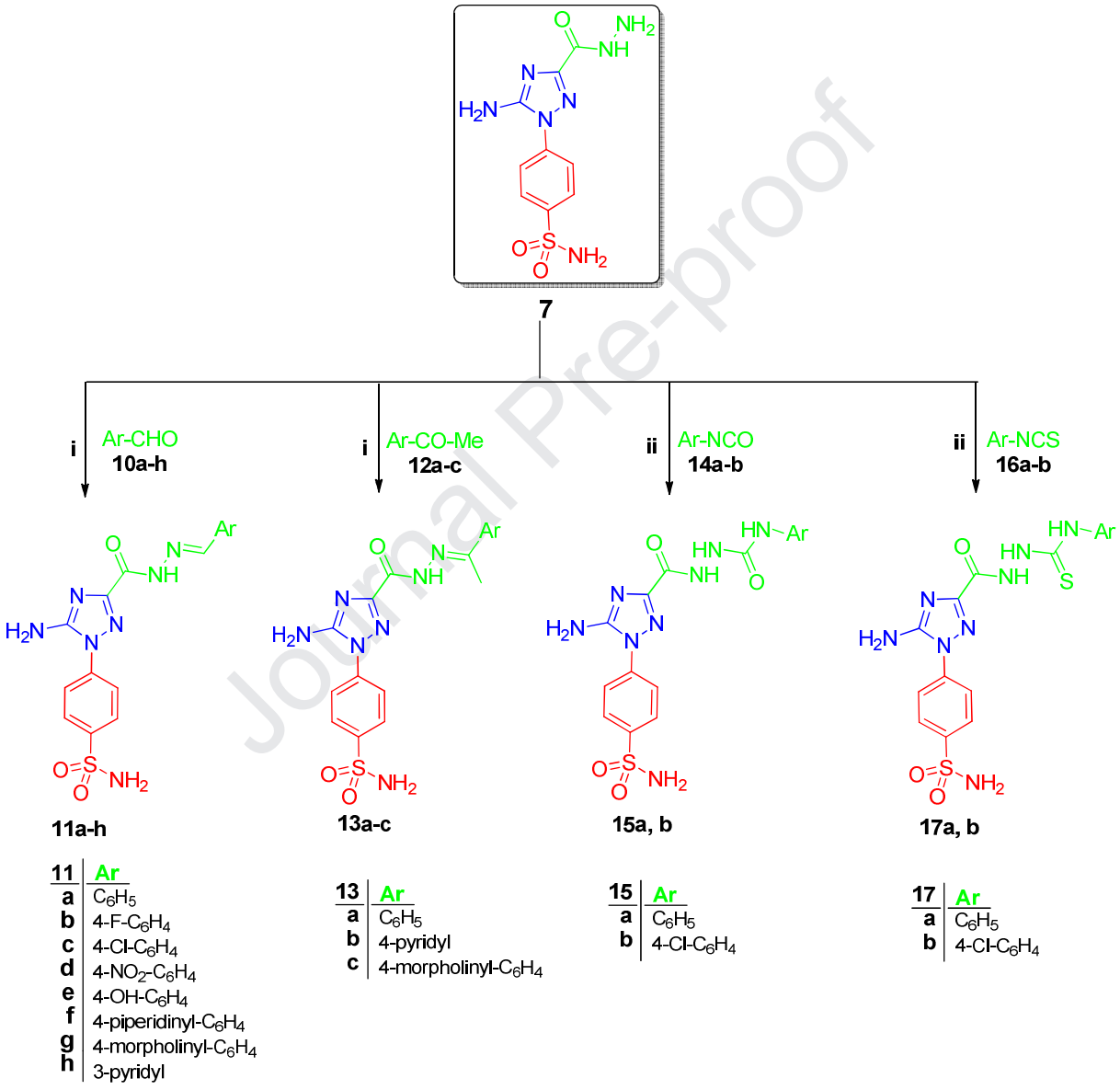

Scheme 3. Reagents and conditions: i. AcOH, reflux 2h; **ii.** Toluene, reflux 3h.

Finally, the target ureides **21a-g** were synthesized through adopting the chemical pathway outlined in **Scheme 4**. Hydrazide **7** was stirred with sodium nitrite in cold glacial acetic acid to

furnish the azide intermediate **18**, which subsequently subjected to Curtius rearrangement through heating in dry xylene to produce the corresponding isocyanate derivative **19**. The target ureido triazole-based benzenesulfonamides **21a-g** were obtained by reaction of isocyanate **19** with different substituted anilines **20a-g** in xylene with 44–60% yield (**Scheme 4**).

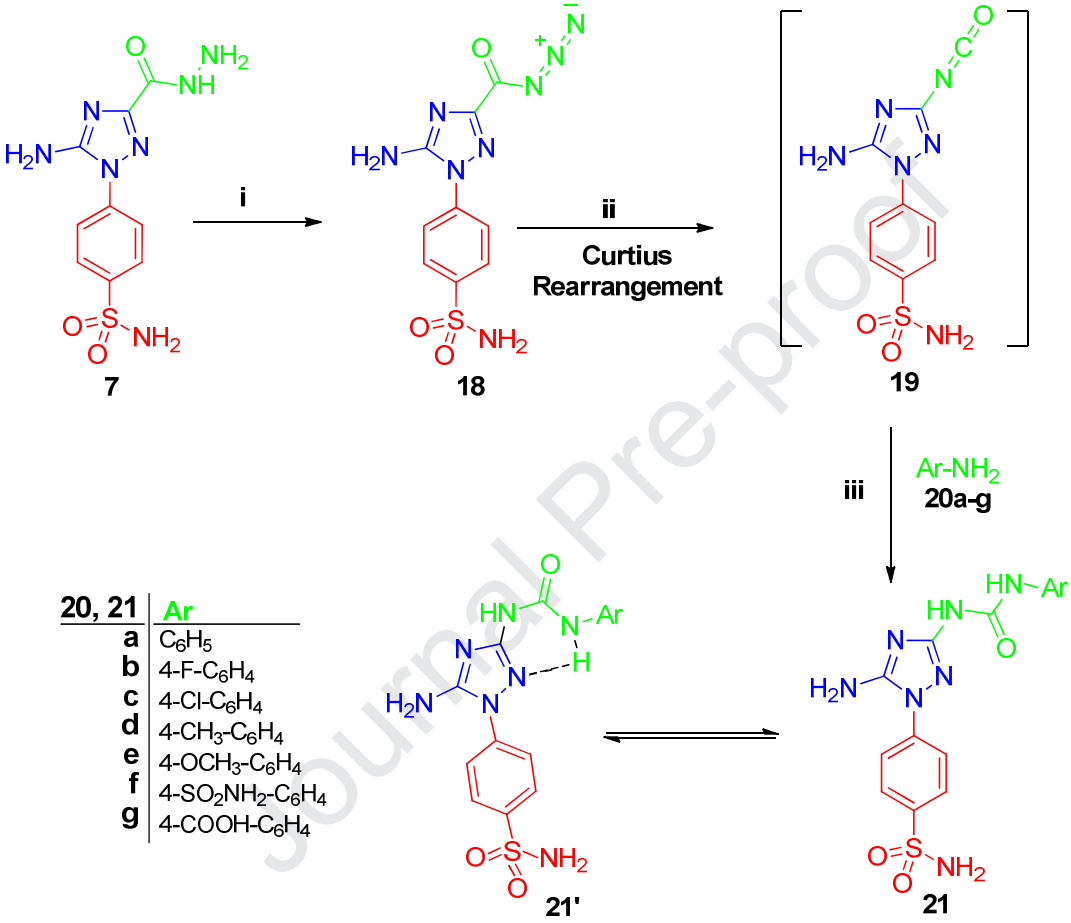

Scheme 4. Reagents and conditions: i. $NaNO_2$, AcOH, stirring 2 h 0 °C; **ii.** Xylene, reflux 1 h; **iii.** Xylene, reflux 3 h.

The structures of the newly synthesized sets of triazolopyrimidine-based (**9a-d**) and triazole-based benzenesulfonamides (**11a-h, 13a-c**, **15a,b**, **17a,b** and **21a-g**) were confirmed under the basis of spectral and elemental analyses which were in full agreement with the postulated structures.

It is noteworthy that, the ^{1}H NMR spectra of target ureides **21a-g** indicated their presence in two geometrical conformations (*Z,Z*, **21**) and (*E,Z*, **21'**), where the first geometrical isomer is the well-known stable form of the ureide derivatives and the other isomer is assumed to be stabilized

by intramolecular hydrogen bonding between one of the ureide hydrogens and N-2 atom of the triazole ring (**Scheme 4**).[20-22] The spectra revealed the presence of two exchangeable singlets corresponding to the NH_2 protons of triazole moiety at δ 6.86- 6.88 *ppm* and 6.99-7.01 *ppm*, beside two other exchangeable singlets corresponding to the NH_2 protons of the sulfonamide group at δ 7.34-7.47 and 7.44-7.53 *ppm*. Compounds **21d** and **21e** spectra showed the presence of two singlets for the methyl protons at δ 2.25 and 2.27 *ppm*, as well as two singlet signals for the methoxy protons at δ 3.73 and 3.75 *ppm*, respectively.

2.2. Biological Evaluation

2.2.1. Carbonic anhydrase inhibition

Six newly prepared triazolopyrimidine-based benzenesulfonamides (**5**, **6** and **9a-d**) as well as twenty three triazole-based benzenesulfonamides (**7**, **11a-h, 13a-c**, **15a,b**, **17a,b** and **21a-g**) were examined for their ability to inhibit the physiologically relevant hCA isoforms, hCA I and II (cytosolic) as well as the tumor associated hCA isoforms hCA IX and XII (trans membrane) through a stopped flow CO_2 hydrase assay [23] using acetazolamide (**AAZ**) as a standard inhibitor. The following structure–activity relationship (SAR) can be concluded from the inhibition data presented in **Table 1**.

(**i**) All the tested sulfonamides showed weak inhibitory effect on the slow cytosolic isoform, hCA I, where the binding affinity constant (K_I) values of twenty-eight compounds out of the twenty-nine tested compounds are fluctuating in the hundreds and thousands nM range (K_I 295.2-4953.5 nM). Only one compound **21b** showed moderate inhibition with K_I value of 94.4 nM.

(**ii**) The physiologically relevant isoform, hCA II, was much more inhibited by most of the tested compounds (K_Is: 6.9-837.6 nM). It is clearly observed that, the triazole-based compounds (**7**, **11a-h**, **13a-c**, **15a**,**b**, **17a**,**b** and **21a-g**) were more potent hCA II inhibitors (K_Is: 6.9-126.6 nM) than the triazolopyrimidine-based drivatives (**5**, **6** and **9a-d**) (K_Is: 74.4-837.6 nM). This difference in the activities of the bicyclic and monocyclic structures is markedly detected by comparing the activity of the triazolopyrimidine hydrazide **6** (K_I = 74.7 nM) with that of its triazole analogue **7** (K_I = 19.9 nM), and by comparing the binding affinities (K_Is: 324.6-837.6) of triazolopyrimidines **9a-d** with the binding affinities (K_Is: 6.6-95.4 nM) of triazoles **11a-h**.

Table 1: Inhibition data of CA isoforms I, II, IX and XII with sulfonamides (**5**, **6**, **7**, **9a-d, 11a-h, 13a-c**, **15a,b**, **17a,b** and **21a-g**), using AAZ as a standard inhibitor.

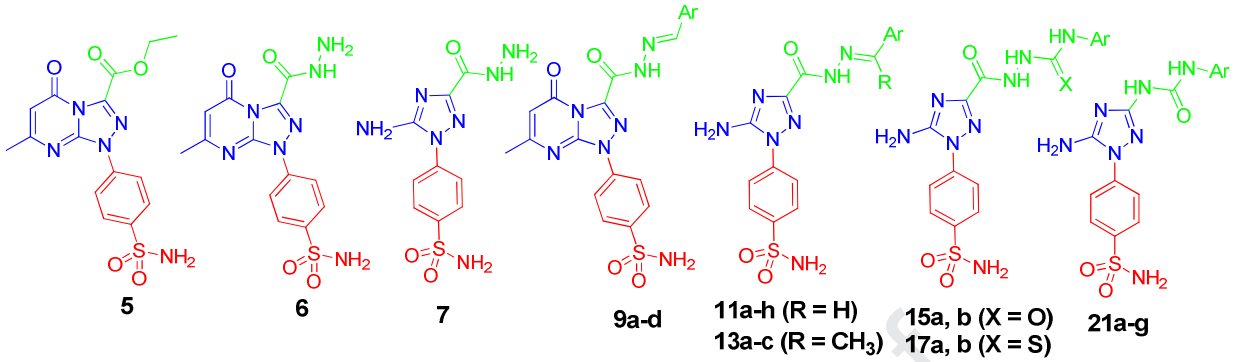

Comp.	R	K_I (nM)			
		hCA I	hCA II	hCA IX	hCA XII
5	-	697.7	85.6	35.9	103.9
6	-	1676.8	74.7	45.4	64.3
7	-	522.7	19.9	22.8	29.4
9a	4- OCH_3-C_6H_4	2381.9	324.6	63.2	38.3
9b	4-(4-methylpiperazin-1-yl)-C_6H_4	4953.5	837.6	85.0	26.2
9c	2-pyridyl	3721.8	536.9	47.9	59.3
9d	4-pyridyl	2481.0	456.2	24.6	45.3
11a	C_6H_5	771.4	86.4	41.1	105.0
11b	4-F-C_6H_4	494.9	65.2	31.5	29.5
11c	4-Cl-C_6H_4	702.7	6.9	73.2	8.2
11d	4-NO_2-C_6H_4	1536.5	24.7	34.4	10.2
11e	4-OH-C_6H_4	334.6	8.8	8.3	7.8
11f	4-piperidinyl-C_6H_4	824.6	95.4	33.0	17.6
11g	4-morpholinyl-C_6H_4	987.7	64.2	19.7	49.7
11h	3-pyridyl	476.5	74.2	6.6	34.4
13a	C_6H_5	633.1	8.9	41.3	23.8
13b	4-pyridyl	295.2	8.5	5.8	26.0
13c	4-morpholinyl-C_6H_4	793.4	53.9	31.7	9.9
15a	C_6H_5	306.9	70.5	4.9	16.2
15b	4-Cl-C_6H_4	537.1	10.9	16.4	48.2

17a	C_6H_5	368.2	9.7	40.2	31.0
17b	4-Cl-C_6H_4	597.5	11.1	16.7	21.9
21a	C_6H_5	442.3	9.8	8.2	8.1
21b	4-F-C_6H_4	94.4	65.5	7.8	17.6
21c	4-Cl-C_6H_4	403.3	9.5	43.3	73.6
21d	4-CH_3-C_6H_4	312.6	42.8	3.9	23.8
21e	4-OCH_3-C_6H_4	694.9	126.6	**3.3**	9.8
21f	4-SO_2NH_2-C_6H_4	676.6	78.7	28.6	4.4
21g	4-COOH-C_6H_4	507.4	9.6	15.3	19.9
AAZ		250.0	12.5	25.0	5.7

* Mean from 3 different assays, by a stopped flow technique (errors were in the range of ± 5-10 % of the reported values).

(**iii**) The tumor associated isoform hCA IX was effectively inhibited by all the tested triazolopyrimidine/triazole-based sulfonamides with K_Is ranging from 3.3 nM to 85.0 nM. Superiorly, eight triazole-based tested sulfonamides emerged as the most potent counterparts against hCA IX isoform in this study with single-digit nanomolar inhibitory activities; **11e** (8.3 nM), **11h** (6.6 nM), **13b** (5.8 nM), **15a** (4.9 nM), **21a** (8.2 nM), **21b** (7.8 nM), **21d** (3.9 nM) and **21e** (3.3 nM). Moreover, sulfonamides **11g**, **15b**, **17b** and **21g** showed better binding affinities (K_Is: 15.3-19.7 nM) than the standard inhibitor **AAZ** (K_I = 25.0 nM). In addition, sulfonamides **7**, **9d** and **21f** showed comparable inhibitory activity (K_I = 22.8, 24.6 and 28.6 nM, respectively) to AAZ toward hCA IX. Notably, among the tested triazole-based sulfonamides, the ureides series **21** stood out as the most promising one, with binding affinities better than (K_Is: 3.3-15.3 nM) or comparable to (K_I = 28.6 nM) the standard inhibitor **AAZ** (K_I = 25.0 nM), except sulfonamide **21c** whose efficacy raised at slightly higher concentration (K_I = 43.3 nM).

It is noteworthy, that bioisosteric replacement of the terminal un/substituted phenyl ring in triazolopyrimidine series **9** (K_Is = 63.2 and 85.0 nM) and triazole series **11** (K_Is: 8.3-73.2 nM) and **13** (K_Is = 41.3 and 31.7 nM) with the hetero pyridyl moiety enhanced the inhibitory activity toward hCA IX isoform; (K_Is = 47.9 and 24.6 nM, for series **9**), (K_I = 6.6 nM, for series **11**) and (K_I = 5.8 nM, for series **13**). In addition, substitution of the terminal phenyl ring in triazole series **11** with electron-withdrawing groups (**11b** and **11d**; K_Is = 31.5 and 34.4 nM,

respectively), or electron-donating groups (**11e-11g**; K_Is = 8.3, 33.0 and 19.7 nM, respectively) improved hCA IX inhibitory activity in comparison to unsubstituted analogue **11a** (K_I = 41.1 nM), except 4-Cl derivative **11c** which displayed higher K_I value (73.2 nM). Furthermore, grafting an electron-donating group (4-CH_3 **21d** and 4-OCH_3 **21e**; K_Is = 3.9 and 3.3 nM, respectively) within the phenyl group of the ureido triazole-based sulfonamides **21** resulted in an enhancement of activity against hCA IX isoform compared to unsubstituted congener **21a** (K_I = 8.2 nM).

iv) The other tumor associated isoform hCA XII is also effectively inhibited by all the tested triazolopyrimidine-based sulfonamides (K_Is range: 26.2-103.9 nM) and triazole-based sulfonamides (K_Is range: 4.4-105 nM). In particular, six triazole-based tested sulfonamides showed potent binding affinities with single-digit nanomolar K_Is values, **11c** (8.2 nM), **11e** (7.8 nM), **13c** (9.9 nM), **21a** (8.1 nM), **21e** (9.8 nM) and **21f** (4.4 nM). Furthermore, sulfonamides **7**, **9b**, **11b**, **11f**, **13a**, **13b**, **15a**, **17b**, **21b**, **21d** and **21g** displayed potent hCA XII inhibitory activity with K_I values ranging from 16.2 to 29.5 nM.

Concerning hCA XII inhibitory activity of the triazole schiff's bases series **11**, we can conclude that grafting a *para*-substituent within the benzylidene moiety, as in compounds **11b-g**, is more beneficial for the activity (K_Is: 7.8-49.7 nM) than unsubstituted congener **11a** (K_I = 105.0 nM). In addition, bioisosteric replacement of the terminal phenyl ring in sulfonamide **11a** (K_I = 105.0 nM) with the hetero 3-pyridyl moiety, sulfonamide **11h**, led to a 3-fold efficacy enhancement (K_I = 34.4 nM) that may be attributed to an extra hydrogen bonding through the heterocyclic nitrogen atom within the active site. Whereas, similar bioisosteric replacement of the phenyl ring in compound **13a** (K_I = 23.8 nM) with the 4-pyridyl ring led to compound **13b** whose efficacy rose to a slightly higher concentration (K_I = 26 nM), unlike what arose for hCA IX.

It is worth highlighting that substitution of the terminal phenyl ring in ureides series **21** elicits a 1.2-fold to 9.1-fold efficacy worsening against hCA XII, except for compound **21f** with incorporated *p*-sulfamoyl group that displays about 2-fold enhanced activity (K_I = 4.4 nM) than unsubstituted analogue **21a** (K_I = 8.1 nM).

Table 2. Selectivity index (SI) calculated for *h*CA IX and XII over off-targets isoforms (*h*CA I and II) for target sulfonamides (**9a-d, 11a-h, 13a-c, 15a,b, 17a,b** and **21a-g**) reported in the paper, and **AAZ**.

Cmpd	I/IX	I/XII	II/IX	II/XII
9a	37.69	62.19	5.14	8.48
9b	58.28	189.06	9.85	31.97
9c	77.70	62.76	11.21	9.05
9d	100.85	54.77	**18.54**	10.07
11a	18.77	7.35	2.10	0.82
11b	15.71	16.78	2.07	2.21
11c	9.60	85.70	0.09	0.84
11d	44.67	150.64	0.72	2.42
11e	40.31	42.90	1.06	1.13
11f	24.99	46.85	2.89	5.42
11g	50.14	19.87	3.26	1.29
11h	72.20	13.85	11.24	2.16
13a	15.33	26.60	0.22	0.37
13b	50.90	11.35	1.47	0.33
13c	25.03	80.14	1.70	5.44
15a	62.63	18.94	14.39	4.35
15b	32.75	11.14	0.66	0.23
17a	9.16	11.88	0.24	0.31
17b	35.78	27.28	0.66	0.51
21a	53.94	54.60	1.20	1.21
21b	12.10	5.36	8.40	3.72
21c	9.31	5.48	0.22	0.13
21d	80.15	13.13	10.97	1.80
21e	210.58	70.91	**38.36**	12.92
21f	23.66	153.77	2.75	17.89
21g	33.16	25.50	0.63	0.48
AAZ	10.00	43.86	0.50	2.19

(**v**) Concerning the selectivity of action of the newly herein reported sulfonamides, the selectivity index (SI) for *h*CA IX and XII over the off-targets isoforms *h*CA I and II are calculated and listed in **Table 2**. Regarding selectivity towards *h*CA IX and XII over *h*CA I, all the target sulfonamides (**9a-d, 11a-h, 13a-c, 15a,b, 17a,b** and **21a-g**) exhibited moderate to excellent SIs spanning in the range 9.16 – 210.58 and 5.36 – 189.06, respectively.

On the other hand, the triazolopyrimidine-based benzenesulfonamide series **9a-d** displayed good selectivity towards *h*CA IX and XII over *h*CA II with SIs spanning in the range 5.14 – 18.54 and 8.48 – 31.97, respectively. Whereas, only triazole-based benzenesulfonamide derivatives **11h**, **15a**, **21b**, **21d** and **21e** were found to be selective toward *h*CA IX over *h*CA II with SIs equal 11.24, 14.39, 8.40, 10.97 and 38.36, respectively. In addition, triazole-based benzenesulfonamide derivatives **13c**, **15a**, **21e** and **21f** exhibited good selectivity towards *h*CA XII over the off-target isoform *h*CA II with SIs equal 5.44, 4.35, 12.92 and 17.89, respectively.

2.2.2. Computational studies

Triazolopyrimidine-based benzenesulfonamide **9d** and triazole-based benzenesulfonamide **21e** were selected as the most selective for the cancer-associated CAs over the ubiquitous isozymes and were docked into the active site of CAs II, IX and XII. Poses showing the best scoring values and favorable binding interactions were subjected to a MM-GBSA based refinement (**Fig. 2**) and, limited to CA IX and XII, to a cycle of 100 ns molecular dynamics (MD, **Fig. 3-5**).

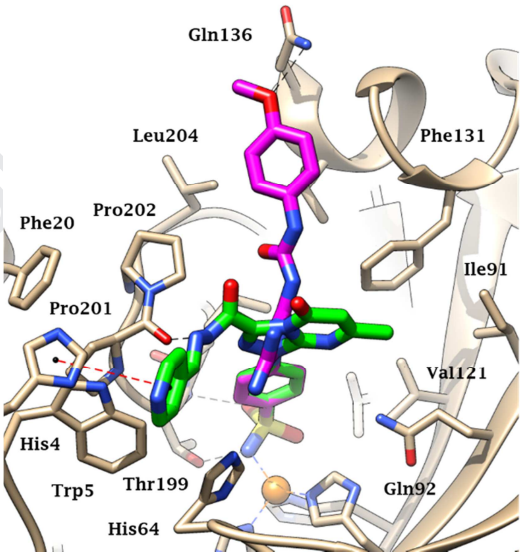

Fig. 2. Docked poses of **9d** (green) and **21e** (magenta) in the active site of CA II. H-Bonds and π-π interactions are depicted as black and red dashed lines, respectively.

In accordance with the X-ray crystallographic reports [24], the benzenesulfonamide fragment of **9d** and **21e** adopted superimposable binding orientations within the three active sites (**Fig. 2**, **4**

and **5**). As a result, the observed specificity of action of the selected compounds needed to be sought in the interactions established by the tails of **9d** and **21e** with the enzymatic counterparts.

While the triazolotriazolopyrimidine of **9d** occupied a central position within the CA II binding pocket, its arylidenehydrazide tail accommodated into the cleft formed by Trp5, His64 and His4, establishing a π-π contact with the latter (**Fig. 2**). Also the 5-amino-1,2,4-triazole portion of **21e** allocated in a middle position of the CA II active site, whereas the 4-methoxyphenylureido tail accommodated in the pocket lined by Leu204, Val135, Phe131 receiving a H-bond by the Gln136 side chain.

The MD simulation undertaken for the two compounds bound to CA IX and XII showed the overall stability of the ligand/target adducts over the tested 100 ns, with the interactions involving the benzenesulfonamide core being steady during the computations (**Fig. 4 and 5**). In contrast, movements of the tails of **9d** and **21e** in relation to the active site residues produced root-mean-square deviation (RMSD), plotted for the ligands heavy atoms as a function of time, which settled in the 2.5-3 Å range for CA IX, and reached 4-6 Å in the case of CA XII (**Fig. 3**). **Figure 4** depicts the main binding orientations reported by **9d** (panel A) and **21e** (panel B) within the binding site of CA IX. The arylidenehydrazide tail of **9d** was found to stably occupy the pocket formed by Val20, Trp5, Pro201 and Pro202 where intense hydrophobic contacts persisted over the MD course (**Fig. 4A**). Additionally, interesting water bridges connecting the pyridine N atom and Val20 carbonyl group and the inner hydrazide N atom and Pro201 C=O, were found for approximately the 20% of the simulation time.

The 4-methoxyphenylureido pendant of **21e** oriented towards a small cleft lined by Leu91, Gln92 and Thr73 and was stabilized by H-bonds persisting for over the 90% of time between Gln92 side chain and the N2 atom of the triazole and the ureido C=O (**Fig. 4B**). Further, two water molecules bridged the oxygen atom of the methoxy group and the Ala90 and Leu74 residues. This network of interaction is present for the 30% of the MD.

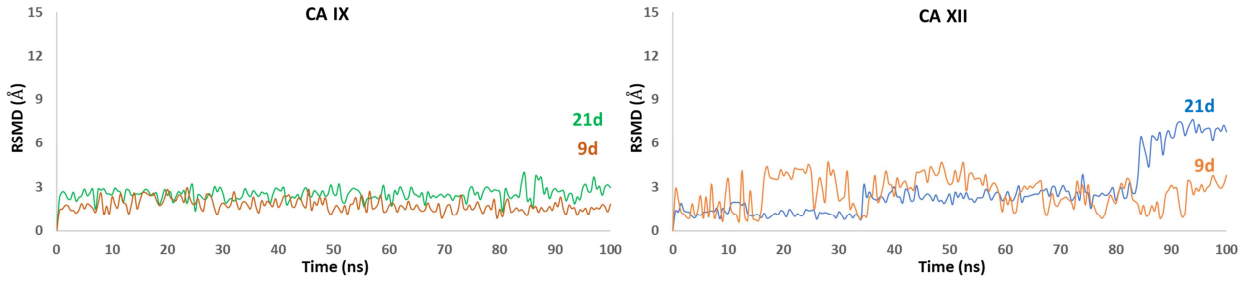

Fig. 3. RMSD analysis of the ligands heavy atoms over the 100 ns MD in CA IX and XII.

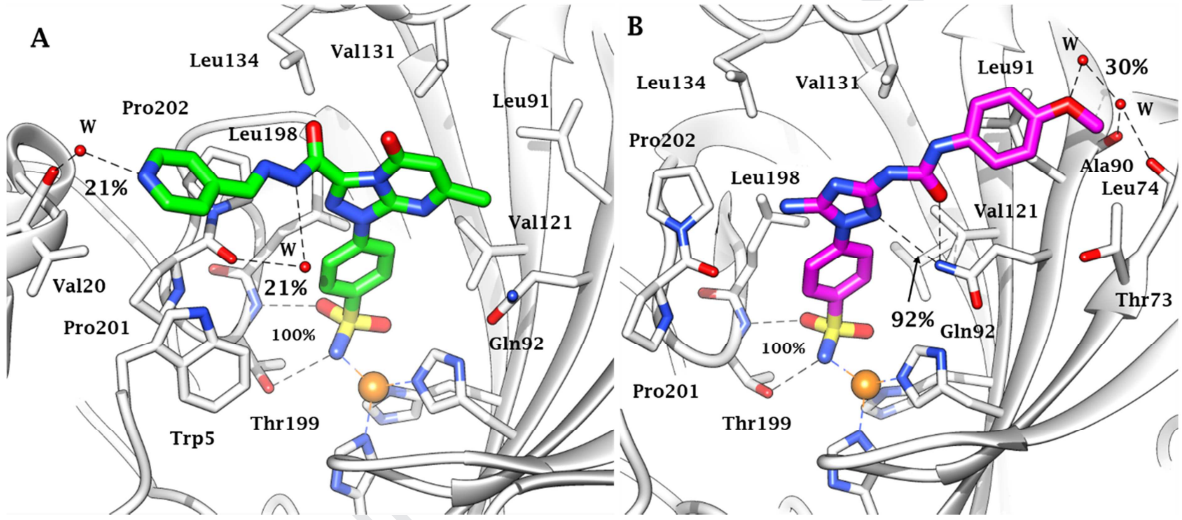

Figure 4. Principal predicted orientation produced over a cycle of 100 ns MD for A) **9d** and B) **21e** bound in the CA IX active site. H-bonds are depicted as black dashed lines. The bond occupancies over 100 ns are reported as percentage.

The binding orientations of the molecular tails of **9d** and **21e** within the CA XII active site were predicted to be less stable in comparison to the CA IX / ligand interactions, as shown in Figure 4. The arylidenehydrazide tail of **9d** established VdW contacts with Tyr20, Pro201 and Pro202, but it did not firmly position into the pocket because of the Val20 (CA IX) / Tyr20 (CA XII) mutation which increases the steric hindrance on the enzymatic counterpart (**Fig. 5A**). As a result, during the MD simulation the arylidenehydrazide tail was found to move within the area comprised from Gln136 to Trp5. The position of the triazolopyrimidine ring was stabilized by π-cation interactions with the ammonium group of Lys67 (30% of the simulation time) whereas a water-mediated interaction between the hydrazido moiety and Gln136 side chain persisted for the 20% of the MD time (**Fig. 5A**).

As far as the adduct of **21e** with CA XII is concerned, the RMSD value plotted as a function of time (**Fig. 3**) indicated that important changes in the ligand binding orientation occurred at approximately 35 and 85 ns of MD (**Fig. 5B**). Indeed, while initially the phenylureido pendant showed to form a H-bond through its ureido C=O with Gln92 (32% of MD time) and a water bridge with Thr91 (with an occasional π-cation interaction with Lys67), after 35 ns the molecular tail shifted toward the α-helix 131-135 only maintaining the water-mediated interaction with Thr91. Approaching to the end of the MD, the phenylureido tail significantly moved away from the original position likely because of H-bonds established by the urea with Ser135 side chain and by the methoxy group with Tyr20 (**Fig. 5B**).

The different binding orientations predicted for both ligands within CA II, IX and XII, allow their selectivity values reported in **Table 2** to be argued. The greater efficacy of **9d** against CA IX than the other isozymes is likely related to the accommodation and strong interaction of the arylidenehydrazide moiety with the aforesaid hydrophobic pocket (Val20, Trp5, Pro201 and Pro202). In fact, the Val20/Phe20 (CA IX/CA II) and the Val20/Tyr20 (CA IX/CA XII) mutations reduced such an intense binding. Nonetheless, in CA XII π-cation interactions of Lys67 with both the benzene and pyridinone rings, not present in CA II, likely led to the increase of K_I values up to a low nanomolar range (**Table 1**).

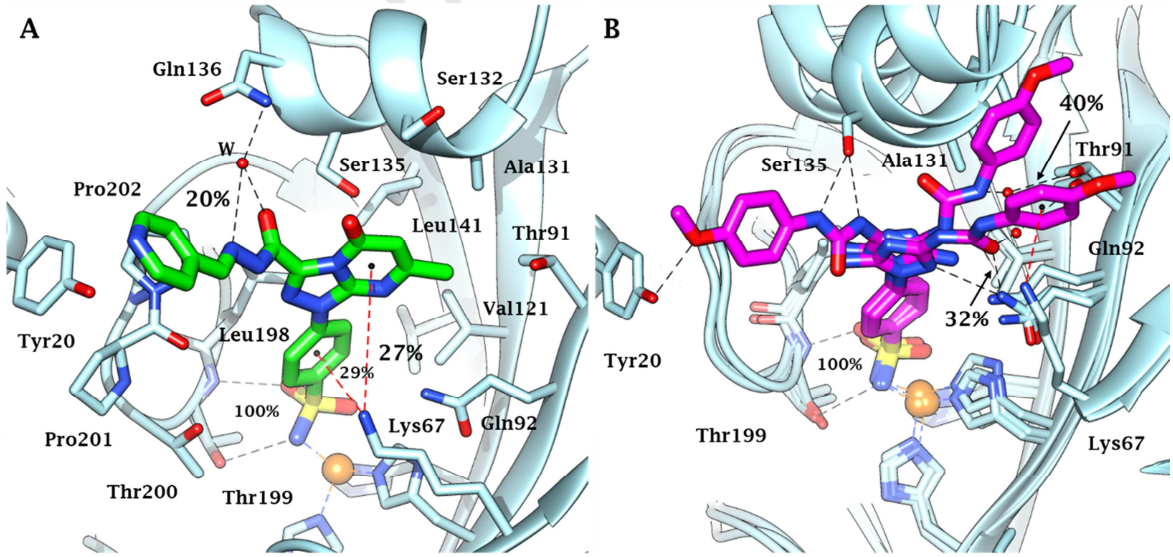

Fig. 5. A) Principal predicted orientation produced over a cycle of 100 ns MD for **9d** bound in the CA XII active site. B) Principal predicted orientations extrapolated from the 100 ns MD of **21e** bound in the CA XII active site. H-Bonds and π-cation interactions are depicted as black and red dashed lines, respectively. The bond occupancies over 100 ns are reported as percentage. The latter are below 10% when not indicated.

In the case of **21e**, the phenylureido tail occupied a different binding pocket in the CA II compared to CA IX and XII (**Fig. 2, 4**, and **5**), presumably owing to the presence of a Phe residue in position 131 which sterically prevent the binding nearby the region where the ligand, in the tumor-associated CAs, bound to Gln92 and Leu91 (CA IX) and Thr91 and Lys67 (CA XII).

3. Conclusion

In summary, we described here the design and synthesis of different new sets of triazolopyrimidine-based (**9a-d**) and triazole-based (**11a-h**, **13a-c**, **15a**,**b**, **17a**,**b** and **21a-g**) benzenesulfonamides as potential CA inhibitors. All the newly synthesized sulfonamides were examined for their inhibitory activities toward *h*CA I, II, IX and XII. The four examined isoforms were inhibited by the prepared sulfonamides (**9a-d**, **11a-h**, **13a-c**, **15a**,**b**, **17a**,**b** and **21a-g**) in variable degrees with K_Is ranges: 94.4-4953.5 nM for hCA I, 6.9-837.6 nM for hCA II, 3.3-85.0 nM for hCA XI, and 4.4-105.0 nM for hCA XII. In particular, sulfonamides **11e, 21a** and **21e** emerged as single-digit nanomolar hCA IX and hCA XII inhibitors. Interestingly, triazolopyrimidine-based sulfonamide **9d** and triazole-based sulfonamide **21e** were found to be the most selective *h*CA IX inhibitors over *h*CA I (SI = 100.85 and 210.58, respectively) and *h*CA II (SI = 18.54 and 38.36, respectively). Docking and molecular dynamics simulations shed light on the ligands selectivity for the cancer-associated CAs over CA II. The great inhibition activity of **9d** against CA IX was attributed to strong interactions the arylidenehydrazide moiety forms with the hydrophobic pocket lined by Val20, Trp5, Pro201 and Pro202, which are absent in CAs II and XII. Nonetheless, π-cation interactions of Lys67 with both the benzene and pyridinone rings of the ligand occur in CA XII (and not in CA II) which increase the K_I values up to a low nanomolar range against the second cancer-related CA.

4. Experimental

4.1. Chemistry

4.1.1. General

Melting points were measured with a Stuart melting point apparatus and were uncorrected. Infrared spectra were recorded as KBr disks on Schimadzu FT-IR 8400S spectrophotometer and expressed in wave number (cm^{-1}). The NMR spectra were recorded by Bruker spectrometer. ^{1}H NMR spectra were run at 400 MHz, while ^{13}C NMR spectra were run at 100 MHz in deuterated dimethylsulfoxide (DMSO-*d6*). All coupling constant (*J*) values are given in hertz. Chemical shifts (δ_H) and (δ_C) are reported relative to DMSO-*d6* as internal standards High-resolution mass spectra were recorded using a Bruker MicroTOF spectrometer. Elemental analyses were carried out at the Regional Center for Microbiology and Biotechnology, Al-Azhar University, Cairo, Egypt.

*4.1.1.1. Synthesis of 6-methyl-2-thioxo-2,3-dihydropyrimidin-4(1H)-one (**2**).*

Compound (2) was synthesized as reported previously [17]. Yield (88%); white powder; m.p. 287–290 °C as reported [17, 25]

*4.1.1.2. Synthesis of ethyl 7-methyl-5-oxo-1-(4-sulfamoylphenyl)-1,5-dihydro-[1,2,4]triazolo[4,3-a]pyrimidine-3-carboxylate (**5**).*

The mixture of 6-methyl-2-thiouracil **2** (1.42 g, 0.01 mol), hydrazonoyl chloride **3** (3 g, 0.01 mol) and triethylamine (1.4 mL, 0.01 mol) in dioxane (30 mL) was heated under reflux for 12h. After cooling, the precipitated solid was collected by filtration, dried and recrystallized from acetonitrile to afford ester **5**. Yield (41%); yellow powder; m.p. 216-218 °C; IR: 3410, 3348 (NH_2), 1735, 1705 (2C=O), 1342, 1165 (SO_2); ^{1}H NMR δ *ppm*: 1.32 (t, 3H, CH_3, *J* = 7.2 Hz), 2.34 (s, 3H, CH_3), 4.45 (q, 2H, CH_2, *J* = 7.2 Hz), 6.02 (s, 1H, H-6 of triazolopyrimidine), 7.47 (s, 2H, NH_2), 7.99 (d, 2H, Ar-H, *J* = 8.8 Hz), 8.28 (d, 2H, Ar-H, *J* = 8.8 Hz); Anal. Calcd. for $C_{15}H_{15}N_5O_5S$ (377.38): C, 47.74; H, 4.01; N, 18.56; found C, 47.34; H, 3.94; N, 18.66.

*4.1.1.3. Synthesis of 4-(3-(hydrazinecarbonyl)-7-methyl-5-oxo-[1,2,4]triazolo[4,3-a]pyrimidin-1(5H)-yl)benzenesulfonamide (**6**)*

To a suspension of ester **5** (3.77 g, 0.01 mol) in ethanol (20 mL), 99% hydrazine hydrate (1 mL, 0.02 mol) was added. The reaction mixture was heated under reflux for 2h, then left to cool. The precipitated product was filtered, washed with water, dried and recrystallized from ethanol to furnish hydrazide **6**. Yield (30%); white powder; m.p. 260-262 °C; IR: 3363, 3309, 3213 (NH,

$2NH_2$), 1716, 1689 (2C=O), 1342, 1157 (SO_2); ^{1}H NMR *δ ppm*: 2.39 (s, 3H, CH_3), 4.87 (s, 2H, -NH_2), 6.09 (s, 1H, H-6 of triazolopyrimidine), 7.52 (s, 2H, -SO_2NH_2), 8.05 (d, 2H, Ar-H, *J* = 8.8 Hz), 8.35 (d, 2H, Ar-H, *J* = 8.8 Hz), 10.52 (s, 1H, -NH); Anal. Calcd. for $C_{13}H_{13}N_7O_4S$ (363.35): C, 42.97; H, 3.61; N, 26.98; found C, 43.09; H, 3.54; N, 27.08.

*4.1.1.4. Synthesis of 4-(5-amino-3-(hydrazinecarbonyl)-1H-[1,2,4]triazol-1-yl)benzenesulfonamide (**7**)*

Excess 99% hydrazine hydrate (5 mL, 0.10 mol) was added to a suspension of ester **5** (3.77 g, 0.01mol) in ethanol (10 mL). The reaction mixture was heated under reflux for 8h. The solid product obtained upon cooling was filtered off, washed several times with water, dried and recrystallized from dioxane to give hydrazide **7**. Yield (33%); white powder; m.p. 254-256 °C; IR: 3464, 3363, 3298, 3251, 3174 (NH, $3NH_2$), 1681 (C=O), 1338, 1161 (SO_2); ^{1}H NMR *δ ppm*: 4.51 (s, 2H, -NH_2 of hydrazide), 6.82 (s, 2H, -NH_2 of triazole), 7.51 (s, 2H, -SO_2NH_2), 7.79 (d, 2H, Ar-H, *J* = 8.8 Hz), 7.96 (d, 2H, Ar-H, *J* = 8.8 Hz), 9.44 (s, 1H, -NH of hydrazide); HRMS (ESI) for $C_9H_{12}O_3N_7{}^{32}S$, calcd 298.07168, found 298.07171 $[M+H]^+$.

*4.1.1.5. Synthesis of 4-(3-(2-(aryl)hydrazine-1-carbonyl)-7-methyl-5-oxo-[1,2,4]triazolo[4,3-a]pyrimidin-1(5H)-yl)benzenesulfonamide (**9a-d**)*

A mixture of equimolar quantities of the previously prepared hydrazide **6** (0.726 g, 0.002 mol) and the appropriate aldehyde **8a-d** (0.002 mol) in absolute ethyl alcohol (10 mL) containing catalytic amount of glacial acetic acid was heated under reflux for 2h, and then cooled to room temperature. The precipitates formed were collected by filtration, dried and crystallized from EtOH/DMF to afford compounds **9a-d**.

*4.1.1.5.1. 4-(3-(2-(4-Methoxybenzylidene)hydrazine-1-carbonyl)-7-methyl-5-oxo-[1,2,4]triazolo[4,3-a]pyrimidin-1(5H)-yl)benzenesulfonamide (**9a**)*

Yield (61%); white powder; m.p. 284–286 °C; IR: 3410, 3332, 3232 (NH, NH_2), 1685, 1604 (2C=O), 1340, 1165 (SO_2); ^{1}H NMR *δ ppm*: 2.42 (s, 3H, CH_3 of triazolopyrimidine), 3.73, 3.83 (2s, 3H, OCH_3), 6.03, 6.13 (2s, 1H, H-6 of triazolopyrimidine), 6.86, 7.05 (2d, 2H, Ar-H, *J* = 8.4 Hz), 7.32, 7.76 (2d, 2H, Ar-H, *J* = 8.4 Hz), 7.53, 7.55 (2s, 2H, NH_2), 8.04, 8.28 (2s, 1H, CH=N-), 8.06 (t, 2H, Ar-H, *J* = 8.4 Hz), 8.40 (t, 2H, Ar-H, *J* = 8.8 Hz), 12.61, 12.68 (2s, 1H, NH); ^{13}C NMR *δ ppm*: 24.67, 24.82 (CH_3), 55.72, 55.83 (OCH_3), 101.23, 101.59, 114.78, 114.89, 120.76,

121.25, 126.31, 126.49, 127.25, 127.64, 129.02, 129.76, 138.55, 138.99, 139.22, 142.77, 143.10, 143.43, 146.46, 147.48, 147.94, 150.43, 151.79, 155.15, 155.93, 158.45, 161.44, 161.88, 167.56, 167.58; Anal. Calcd. for $C_{21}H_{19}N_7O_5S$ (481.49): C, 52.39; H, 3.98; N, 20.36; found C, 52.49; H, 3.93; N, 20.27.

*4.1.1.5.2. 4-(7-Methyl-3-(2-(4-(4-methylpiperazin-1-yl)benzylidene)hydrazine-1-carbonyl)-5-oxo-[1,2,4]triazolo[4,3-a]pyrimidin-1(5H)-yl)benzenesulfonamide (**9b**)*

Yield (64%); yellow powder; m.p. 288–290 °C; IR: 3367, 3298, 3194 (NH, NH_2), 1695, 1685 (2C=O), 1346, 1165 (SO_2); ^{1}H NMR *δ ppm*: 1.92 (s, 3H, CH_3 of methyl piprazine), 2.18, 2.23 (2 br.s, 4H, H-3, H-5 of methyl piprazine), 2.38, 2.45 (2s, 3H, CH_3 of triazolopyrimidine), 3.16, 3.27 (2 br.s, 4H, H-2, H-6 of methyl piprazine), 6.02, 6.12 (2s, 1H, H-6 of triazolopyrimidine), 6.81, 7.00 (2d, 2H, Ar-H, *J* = 8.4 Hz), 7.18, 7.63 (2d, 2H, Ar-H, *J* = 8.4 Hz), 7.54 (br s, 2H, NH_2), 7.96, 8.18 (2s, 1H, CH=N-), 8.05 (t, 2H, Ar-H, *J* = 8.0 Hz), 8.39 (t, 2H, Ar-H, *J* = 9.6Hz), 12.60 (br s, 1H, NH); ^{13}C NMR *δ ppm*: 21.58 (CH_3 of triazolopyrimidine), 24.66, 24.81 (CH_3 of methyl piprazine), 46.06, 46.11, 47.29, 47.31, 47.45, 54.67, 54.77 (piprazine carbons), 101.26, 101.58, 114.78, 120.72, 121.17, 123.37, 123.79, 127.59, 128.57, 129.38, 138.63, 139.00, 139.08, 139.20, 142.75, 143.06, 146.86, 147.44, 147.92, 150.82, 151.57, 152.58, 152.96, 155.14, 155.96, 158.23, 167.57, 167.72, 172.62, 172.76; Anal. Calcd. for $C_{25}H_{27}N_9O_4S$ (549.61): C, 54.63; H, 4.95; N, 22.94; found C, 54.93; H, 4.88; N, 22.84.

*4.1.1.5.3. 4-(7-Methyl-5-oxo-3-(2-(pyridin-2-ylmethylene)hydrazine-1-carbonyl)-[1,2,4]triazolo[4,3-a]pyrimidin-1(5H)-yl)benzenesulfonamide (**9c**)*

Yield (60%); white powder; m.p. 290–292 °C; IR: 3498, 3356, 3236 (NH, NH_2), 1695, 1670 (2C=O), 1330, 1165 (SO_2); ^{1}H NMR *δ ppm*: 2.40, 2.41 (2s, 3H, CH_3 of triazolopyrimidine), 6.02, 6.13 (2s, 1H, H-6 of triazolopyrimidine), 7.33-7.40, 7.48-7.54 (2m, 4H, 2H Ar-H and 2H, NH_2), 7.67, 7.93 (2t, 1H, Ar-H, *J* = 7.6 Hz), 8.07 (t, 2 H, Ar-H, *J* = 7.8 Hz), 8.13, 8.33 (2s, 1H, CH=N-), 8.39 (t, 2H, Ar-H, *J* = 9.4 Hz), 8.55, 8.66 (2d, 1H, Ar-H, *J* = 4.8 Hz), 12.92 (s, 1H, NH); Anal. Calcd. for $C_{19}H_{16}N_8O_4S$ (452.45): C, 50.44; H, 3.56; N, 24.77; found C, 50.14; H, 3.59; N, 24.87.

*4.1.1.5.4. 4-(7-Methyl-5-oxo-3-(2-(pyridin-4-ylmethylene)hydrazine-1-carbonyl)-[1,2,4]triazolo[4,3-a]pyrimidin-1(5H)-yl)benzenesulfonamide (**9d**)*

Yield (57%); white powder; m.p. 289–291°C; IR: 3421, 3305, 3221 (NH, NH_2), 1689, 1670 (2C=O), 1350, 1165 (SO_2); ^{1}H NMR *δ ppm*: 2.42 (s, 3H, CH_3 of triazolopyrimidine), 6.03, 6.15 (2s, 1H, H-6 of triazolopyrimidine 7.34, 7.75 (2d, 2H, Ar-H, *J* = 5.6 Hz), 7.52, 7.54 (2s, 2H, NH_2), 8.05 (t, 2H, Ar-H, *J* = 9.2 Hz), 8.36 (s, 1H, CH=N-), 8.39 (t, 2H, Ar-H, *J* = 9.2 Hz), 8.51, 8.71 (2d, 2H, Ar-H, *J* = 5.2 Hz), 13.01, 13.03 (2s, 1H, NH); Anal. Calcd. for $C_{19}H_{16}N_8O_4S$ (452.45): C, 50.44; H, 3.56; N, 24.77; found C, 50.64; H, 3.58; N, 24.67.

*4.1.1.6. Synthesis of target sulfonamides (**11a-h** and **13a-c**)*

A mixture of equimolar quantities of triazole-based hydrazide **7** (0.59 g, 0.002 mol) and the appropriate aldehyde **10a-h** (0.002 mol) or the appropriate acetophenone **12a-c** (0.002 mol) in glacial acetic acid (5 mL) was refluxed for 2h, and then cooled to room temperature. The formed precipitate was collected by filtration, dried and recrystallized from EtOH/DMF to afford target compounds **11a-h** and **13a-c**, respectively.

*4.1.1.6.1. 4-(5-Amino-3-(2-benzylidenehydrazine-1-carbonyl)-1H-1,2,4-triazol-1-yl)benzenesulfonamide (**11a**)*

Yield (66%); white powder; m.p. 283–285 °C; IR: 3479, 3421, 3275, 3186, 3140 (NH, $2NH_2$), 1685 (C=O), 1327, 1153 (SO_2); ^{1}H NMR *δ ppm*: 6.94 (s, 2H, NH_2), 7.47-7.74 (m, 7H, 2H of -SO_2NH_2 and 5H, Ar-H), 7.87 (d, 2H, Ar-H, *J* = 8 Hz), 8.03 (d, 2H, Ar-H, *J* = 8 Hz), 8.57 (s, 1H, CH=N-), 11.80 (s, 1H, NH); ^{13}C NMR *δ ppm*: 123.56, 127.59, 127.66, 129.33, 130.70, 134.69, 139.59, 143.46, 149.17, 154.35, 156.04, 156.18; Anal. Calcd. for $C_{16}H_{15}N_7O_3S$ (385.40): C, 49.86; H, 3.92; N, 25.44; found C, 50.13; H, 3.89; N, 25.35.

*4.1.1.6.2. 4-(5-Amino-3-(2-(4-fluorobenzylidene)hydrazine-1-carbonyl)-1H-1,2,4-triazol-1-yl)benzenesulfonamide (**11b**)*

Yield (64%); white powder; m.p. 293–295 °C; IR: 3475, 3421, 3278, 3120 (NH, $2NH_2$), 1689 (C=O), 1327, 1153 (SO_2); ^{1}H NMR *δ ppm*: 6.90 (s, 2H, NH_2), 7.29 (t, 2H, Ar-H, *J* = 8.8 Hz), 7.54 (s, 2H, -SO_2NH_2), 7.76 (dd, 2H, Ar-H, *J* = 8.0 Hz, *J* = 5.6 Hz), 7.84 (d, 2H, Ar-H, *J* = 8.4 Hz), 7.80 (d, 2H, Ar-H, *J* = 8.4 Hz), 8.54 (s, 1H, CH=N-), 11.78 (s, 1H, NH); Anal. Calcd. for $C_{16}H_{14}FN_7O_3S$ (403.39): C, 47.64; H, 3.50; N, 24.31; found C, 47.29; H, 3.47; N, 24.39.

*4.1.1.6.3. 4-(5-Amino-3-(2-(4-chlorobenzylidene)hydrazine-1-carbonyl)-1H-1,2,4-triazol-1-yl)benzenesulfonamide (**11c**)*

Yield (70%); white powder; m.p. 285-287 °C; IR: 3410, 3367, 3298, 3259 (NH, $2NH_2$), 1678 (C=O), 1338, 1157 (SO_2); ^{1}H NMR *δ ppm*: 6.91 (s, 2H, NH_2), 7.53-7.55 (m, 4H, 2H, Ar-H and 2H, SO_2NH_2, D_2O exchangeable), 7.73 (d, 2H, Ar-H, *J* = 8 Hz), 7.85 (d, 2H, Ar-H, *J* = 8 Hz), 8.00 (d, 2H, Ar-H, *J* = 8.4 Hz), 8.54 (s, 1H, CH=N-), 11.84 (s, 1H, NH); HRMS (ESI) for $C_{16}H_{15}O_3N_7{}^{35}Cl^{32}S$, calcd 420.06401, found 420.06390 $[M+H]^+$.

*4.1.1.6.4. 4-(5-Amino-3-(2-(4-nitrobenzylidene)hydrazine-1-carbonyl)-1H-1,2,4-triazol-1-yl)benzenesulfonamide (**11d**)*

Yield (69%); buff powder; m.p. 296–298 °C; IR: 3471, 3379, 3221, 3194 (NH, $2NH_2$), 1693 (C=O), 1338, 1165 (SO_2); ^{1}H NMR *δ ppm*: 6.94 (s, 2H, NH_2), 7.56 (s, 2H, -SO_2NH_2), 7.86 (d, 2H, Ar-H, *J* = 7.2 Hz), 7.97, 8.03 (2d, 4H, Ar-H, *J* = 7.6 Hz), 8.31 (d, 2H, Ar-H, *J* = 7.2 Hz), 8.66 (s, 1H, CH=N-), 12.11 (s, 1H, NH); ^{13}C NMR *δ ppm*: 123.52, 124.54, 125.78, 127.57, 139.51, 141.01, 143.54, 146.60, 148.38, 154.10, 156.09, 156.36; Anal. Calcd. for $C_{16}H_{14}N_8O_5S$ (430.40): C, 44.65; H, 3.28; N, 26.04; found C, 44.83; H, 3.34; N, 26.09.

*4.1.1.6.5. 4-(5-Amino-3-(2-(4-hydroxybenzylidene)hydrazine-1-carbonyl)-1H-1,2,4-triazol-1-yl)benzenesulfonamide (**11e**)*

Yield (70%); buff powder; m.p. >300 °C; IR: 3433, 3271, 3217, 3155, 3136, 3116 (OH, NH, $2NH_2$), 1681 (C=O), 1334, 1165 (SO_2); ^{1}H NMR *δ ppm*: 6.91 (br s, 4H, 2H, Ar-H and 2H of NH_2), 7.58-8.04 (m, 8H, 2H of SO_2NH_2 and 6H, Ar-H), 8.46 (s, 1H, CH=N-), 10.00 (s, 1H, OH), 11.59 (s, 1H, NH); ^{13}C NMR *δ ppm*: 116.20, 123.81, 125.69, 127.54, 129.44, 139.60, 143.39, 149.34, 154.51, 155.85, 155.95, 159.98; Anal. Calcd. for $C_{16}H_{15}N_7O_4S$ (401.40): C, 47.88; H, 3.77; N, 24.43; found C, 48.18; H, 3.83; N, 24.53.

*4.1.1.6.6. 4-(5-Amino-3-(2-(4-(piperidin-1-yl)benzylidene)hydrazine-1-carbonyl)-1H-1,2,4-triazol-1-yl)benzenesulfonamide (**11f**)*

Yield (66%); buff powder; m.p. 298–300 °C; IR: 3460, 3417, 3367, 3278, 3259 (NH, $2NH_2$), 1678 (C=O), 1330, 1161 (SO_2); ^{1}H NMR *δ ppm*: 1.578 (br s, 6H, H-3, H-4 and H-5 of piperidine), 3.27 (br s, 4H, H-2, H-6 of piperidine), 6.90 (s, 2H, NH_2), 6.96 (d, 2H, Ar-H, *J* = 8.4

Hz), 7.53-7.56 (m, 4H, 2H Ar-H and 2H SO_2NH_2, D_2O exchangeable), 7.86 (d, 2H, Ar-H, *J* = 8.4 Hz), 8.01 (d, 2H, Ar-H, *J* = 8.4 Hz), 8.40 (s, 1H, CH=N-), 11.49 (s, 1H, NH); ^{13}C NMR *δ ppm*: 24.39 (C-4 of piperidine), 25.43 (C-3 and C-5 of piperidine), 48.84 (C-2 and C-6 of piperidine), 115.00, 123.48, 123.76, 127.56, 128.71, 139.63, 143.16, 149.53, 152.91, 154.53, 155.94, 159.10; Anal. Calcd. for $C_{21}H_{24}N_8O_3S$ (468.54): C, 53.83; H, 5.16; N, 23.92; found C, 53.55; H, 5.11; N, 23.82.

*4.1.1.6.7. 4-(5-Amino-3-(2-(4-morpholinobenzylidene)hydrazine-1-carbonyl)-1H-1,2,4-triazol-1-yl)benzenesulfonamide (**11g**)*

Yield (58%); buff powder; m.p. 297–300 °C; IR: 3452, 3309, 3259, 3186, 3143 (NH, $2NH_2$), 1685 (C=O), 1323, 1153 (SO_2); ^{1}H NMR *δ ppm*: 3.22 (br.s, 4H, H-2, H-6 of morpholine), 3.75 (br.s, 4H, H-3, H-5 of morpholine), 6.89 (s, 2H, NH_2), 7.00 (d, 2H, Ar-H, *J* = 8.4 Hz), 7.54 (s, 2H, -SO_2NH_2), 7.56 (d, 2H, Ar-H, *J* = 8.4 Hz), 7.84 (d, 2H, Ar-H, *J* = 8.4 Hz), 7.99 (d, 2H, Ar-H, *J* = 8.4 Hz), 8.41 (s, 1H, CH=N-), 11.52 (s, 1H, NH); Anal. Calcd. for $C_{20}H_{22}N_8O_4S$ (470.51): C, 51.06; H, 4.71; N, 23.82; found C, 50.74; H, 4.74; N, 23.92.

*4.1.1.6.8. 4-(5-Amino-3-(2-(pyridin-3-ylmethylene)hydrazine-1-carbonyl)-1H-1,2,4-triazol-1-yl)benzenesulfonamide (**11h**)*

Yield (67%); white powder; m.p. 283–285 °C; IR: 3479, 3417, 3294, 3194, 3101 (NH, $2NH_2$), 1678 (C=O), 1334, 1165 (SO_2); ^{1}H NMR *δ ppm*: 6.93 (s, 2H, NH_2), 7.49-7.56 (m, 3H, H-5 of pyridine and 2H, -SO_2NH_2), 7.86 (d, 2H, Ar-H, *J* = 8.4 Hz), 8.01 (d, 2H, Ar-H, *J* = 8 Hz), 8.13 (d, 1H, H-4 of pyridine, *J* = 7.2 Hz), 8.61-8.64 (m, 2H, 1H of C<u>H</u>=N- and 1H of H-6 of pyridine), 8.84 (s, 1H, H-2 of pyridine), 11.97 (s, 1H, NH); ^{13}C NMR *δ ppm*: 123.52, 124.52, 127.57, 130.64, 134.08, 139.54, 143.16, 146.40, 149.21, 151.26, 154.20, 155.77, 156.24; Anal. Calcd. for $C_{15}H_{14}N_8O_3S$ (386.39): C, 46.63; H, 3.65; N, 29.00; found C, 46.33; H, 3.61; N, 29.10.

*4.1.1.6.9. 4-(5-Amino-3-(2-(1-phenylethylidene)hydrazine-1-carbonyl)-1H-1,2,4-triazol-1-yl)benzenesulfonamide (**13a**)*

Yield (55%); white powder; m.p. 292–294 °C; IR: 3329, 3259, 3228, 3194, 3155 (NH, $2NH_2$), 1701 (C=O), 1346, 1168 (SO_2); ^{1}H NMR *δ ppm*: 2.33 (s, 3H, CH_3), 6.98 (s, 2H, -NH_2), 7.42-7.44

(m, 3H, Ar-H), 7.50 (s, 2H, -SO_2NH_2), 7.81-7.85 (m, 4H, Ar-H), 7.95 (d, 2H, Ar-H, *J* = 8 Hz), 10.39 (s, 1H, -NH); ^{13}C NMR *δ ppm*: 14.08 (CH_3), 123.76, 126.92, 127.56, 128.87, 130.10, 138.17, 139.54, 143.42, 154.28, 154.66, 155.89, 172.45; Anal. Calcd. for $C_{17}H_{17}N_7O_3S$ (399.43): C, 51.12; H, 4.29; N, 24.55; found C, 51.31; H, 4.22; N, 24.63.

*4.1.1.6.10. 4-(5-Amino-3-(2-(1-(pyridin-4-yl)ethylidene)hydrazine-1-carbonyl)-1H-1,2,4-triazol-1-yl)benzenesulfonamide (**13b**)*

Yield (59%); white powder; m.p. 295–297 °C; IR: 3406, 3329, 3271, 3197, 3163 (NH, $2NH_2$), 1697 (C=O), 1350, 1168 (SO_2); ^{1}H NMR *δ ppm*: 2.35 (s, 3H, CH_3), 7.01 (s, 2H, -NH_2), 7.52 (s, 2H, -SO_2NH_2), 7.77 (d, 2H, Ar-H, *J* = 5.6 Hz), 7.82 (d, 2H, Ar-H, *J* = 8.8 Hz), 7.96 (d, 2H, Ar-H, *J* = 8.8 Hz), 8.64 (d, 2H, Ar-H, *J* = 6.0 Hz), 10.56 (s, 1H, -NH); ^{13}C NMR *δ ppm*: 13.59 (CH_3), 121.00, 123.83, 127.58, 139.50, 143.49, 145.22, 150.52, 152.11, 154.08, 155.95, 172.47; HRMS (ESI) for $C_{16}H_{17}O_3N_8{}^{32}S$, calcd 401.11388, found 401.11300 $[M+H]^+$.

*4.1.1.6.11. 4-(5-Amino-3-(2-(1-(4-morpholinophenyl)ethylidene)hydrazine-1-carbonyl)-1H-1,2,4-triazol-1-yl)benzenesulfonamide (**13c**)*

Yield (52%); buff powder; m.p. 299–300 °C; IR: 3456, 3352, 3267 (NH, $2NH_2$), 1681 (C=O), 1323, 1153 (SO_2); ^{1}H NMR *δ ppm*: 2.27 (s, 3H, CH_3), 3.18 (t, 4H, H-3, H-5 of morpholine, *J* = 4.6 Hz), 3.73 (t, 4H, H-2, H-6 of morpholine, *J* = 4.8 Hz), 6.97-7.00 (m, 4H, 2H, Ar-H and 2H, -NH_2), 7.52 (s, 2H, -SO_2NH_2), 7.73 (d, 2H, Ar-H, *J* = 8.8 Hz), 7.81 (d, 2H, Ar-H, *J* = 8.8 Hz), 7.96 (d, 2H, Ar-H, *J* = 8.8 Hz), 10.29 (s, 1H, -NH); ^{13}C NMR *δ ppm*: 13.69 (CH_3), 48.03 (C-3, C-5 of morpholine), 66.43 (C-2, C-6 of morpholine), 114.42, 123.73, 127.56, 127.99, 128.16, 139.59, 143.38, 152.37, 154.43, 154. 84, 155.44, 155.84; Anal. Calcd. for $C_{21}H_{24}N_8O_4S$ (484.54): C, 52.06; H, 4.99; N, 23.13; found C, 52.28; H, 4.96; N, 23.22.

*4.1.1.7. Synthesis of 2-(5-amino-1-(4-sulfamoylphenyl)-1H-1,2,4-triazole-3-carbonyl)-N-(4-substituted)hydrazine-1-carboxamide (**15a, b**) and carbothioamide (**17a, b**)*

To a solution of the appropriate phenyl isocynate **14a**,**b** or phenyl isothiocynate **16a**,**b** (0.001mol) in dry toluene (10 mL), hydrazide **7** (0.3 g, 0.001 mol) was added, and then the reaction mixture was heated under reflux for 3h. The formed precipitate was filtered while hot, and recrystallized from dioxane to afford target sulfonamides **15a**, **b** and **17a**, **b** respectively.

*4.1.1.7.1. 2-(5-Amino-1-(4-sulfamoylphenyl)-1H-1,2,4-triazole-3-carbonyl)-N-phenylhydrazine-1-carboxamide (**15a**)*

Yield (69%); white powder; m.p. 279–281°C; IR: 3406, 3332, 3282, 3178 (3NH, $2NH_2$), 1643, 1562 (2C=O), 1315, 1157 (SO_2); ^{1}H NMR *δ ppm*: 6.86 (s, 2H, -NH_2), 6.92 (t, 1H, Ar-H, *J* = 8.0 Hz), 7.22 (t, 2H, Ar-H, *J* = 8.0 Hz), 7.43 (d, 2H, Ar-H, *J* = 8.0 Hz), 7.49 (s, 2H, -SO_2NH_2), 7.79 (d, 2H, Ar-H, *J* = 8.4 Hz), 7.95 (d, 2H, Ar-H, *J* = 8.8 Hz), 8.18 (s, 1H, -NH), 8.76 (s, 1H, -NH), 9.93 (s, 1H, -NH); ^{13}C NMR *δ ppm*: 118.88, 122.31, 123.63, 127.53, 129.09, 139.62, 140.11, 143.30, 153.97, 155.59, 155.91, 159.69; Anal. Calcd. for $C_{16}H_{16}N_8O_4S$ (416.42): C, 46.15; H, 3.87; N, 26.91; found C, 45.92; H, 3.84; N, 26.81.

*4.1.1.7.2. 2-(5-Amino-1-(4-sulfamoylphenyl)-1H-1,2,4-triazole-3-carbonyl)-N-(4-chlorophenyl)hydrazine-1-carboxamide (**15b**)*

Yield (70%); white powder; m.p. 252–254 °C; IR: 3363, 3302, 3278 3194, 3101 (3NH, $2NH_2$), 1681, 1647 (2C=O), 1307, 1161 (SO_2); ^{1}H NMR *δ ppm*: 6.88 (s, 2H, -NH_2), 7.30 (d, 2H, Ar-H, *J* = 8.8 Hz), 7.51-7.52 (m, 4H, 2H, Ar-H and 2H, -SO_2NH_2), 7.82 (d, 2H, Ar-H, *J* = 8.4 Hz), 7.98 (d, 2H, Ar-H, *J* = 8.4 Hz), 8.30 (s, 1H, -NH), 8.95 (s, 1H, -NH), 9.98 (s, 1H, -NH); Anal. Calcd. for $C_{16}H_{15}ClN_8O_4S$ (450.86): C, 42.62; H, 3.35; N, 24.85; found C, 42.98; H, 3.37; N, 24.76.

*4.1.1.7.3. 2-(5-Amino-1-(4-sulfamoylphenyl)-1H-1,2,4-triazole-3-carbonyl)-N-phenylhydrazine-1-carbothioamide (**17a**)*

Yield (72%); white powder; m.p. 248–250 °C; IR: 3367, 3298, 3251, 3178 (3NH, $2NH_2$), 1678 (C=O), 1338, 1161 (SO_2); ^{1}H NMR *δ ppm*: 6.78 (s, 2H, -NH_2), 7.10 (t, 1H, Ar-H, *J* = 7.2 Hz), 7.28 (t, 2H, Ar-H, *J* = 8.0 Hz), 7.44-7.53 (m, 4H, 2H, Ar-H and 2H, -SO_2NH_2), 7.75 (t, 2H, Ar-H, *J* = 8.4 Hz), 7.92 (t, 2H, Ar-H, *J* = 8.4 Hz), 9.40 (s, 1H, -NH), 9.72 (s, 1H, -NH), 10.25 (s, 1H, -NH); ^{13}C NMR *δ ppm*: 123.44, 123.57, 127.49, 127.56, 139.61, 139.69, 143.10, 143.31, 154.56, 155.71, 155.86, 159.09; HRMS (ESI) for $C_{16}H_{17}O_3N_8{}^{32}S_2$, calcd 433.08595, found 433.08584 $[M+H]^+$.

*4.1.1.7.4. 2-(5-Amino-1-(4-sulfamoylphenyl)-1H-1,2,4-triazole-3-carbonyl)-N-(4-chlorophenyl)hydrazine-1-carbothioamide (**17b**)*

Yield (68%); white powder; m.p. 244–246 °C; IR: 3363, 3298, 3251, 3209, 3140 (3NH, $2NH_2$), 1658 (C=O), 1338, 1161 (SO_2); ^{1}H NMR *δ ppm*: 6.81 (s, 2H, -NH_2), 7.36 (d, 2H, Ar-H, *J* = 8.4 Hz), 7.51-7.52 (m, 4H, 2H, Ar-H and 2H, -SO_2NH_2), 7.79 (t, 2H, Ar-H, *J* = 8.8 Hz), 7.95 (t, 2H, Ar-H, *J* = 8.4 Hz), 9.43 (s, 1H, -NH), 9.79 (s, 1H, -NH), 10.31 (s, 1H, -NH); Anal. Calcd. for $C_{16}H_{15}ClN_8O_3S_2$ (466.92): C, 41.16; H, 3.24; N, 24.00; found C, 41.45; H, 3.29; N, 23.92.

*4.1.1.8. Synthesis of 4-(5-amino-3-(3-(4-(un)substituted phenyl)ureido)-1H-1,2,4-triazol-1-yl)benzenesulfonamide (**21a–g**)*

In an ice bath, a mixture of the hydrazide **7** (1.49 g, 0.005mol) and sodium nitrite (0.5 g, 0.007mol) was stirred in glacial acetic acid for 1h, then stirring was continued at room temperature for another 1h. The obtained solid was collected by filtration, washed with cold water and air-dried to furnish 5-amino-1-(4-sulfamoylphenyl)-1*H*-1,2,4-triazole-3-carbonyl azide **18**, which used in the next reaction without further purification. Then, the appropriate azide was heated under reflux in dry xylene for 1h before addition of anilines **20a-g**. This reaction mixture was refluxed for 3h then allowed to cool to room temperature. The formed precipitate was filtered off, washed with cold acetone, dried and recrystallized from dioxane to furnish the target triazole-based ureides **21a**–**g**.

*4.1.1.8.1. 4-(5-Amino-3-(3-phenylureido)-1H-1,2,4-triazol-1-yl)benzenesulfonamide (**21a**)*

Yield (48%); white powder; m.p. 251–253 °C; IR: 3379, 3321, 3221 (2NH, $2NH_2$), 1685 (C=O), 1334, 1161 (SO_2); ^{1}H NMR *δ ppm*: 6.87-7.02 (m, 3H, 1H Ar -H and 2H, -NH_2 of triazole), 7.28-7.44 (m, 3H, 1 H Ar-H and 2H, -SO_2NH_2), 7.50 (d, 2H, Ar-H, *J* = 7.2 Hz), 7.63-7.76 (m, 2H, Ar-H), 7.82, 7.91 (2d, 2H, Ar-H, *J* = 8.8 Hz), 7.98, 9.74 (2s, 1H, -NH), 10.08, 10.38 (2s, 1H, -NH); Anal. Calcd. for $C_{15}H_{15}N_7O_3S$ (373.39): C, 48.25; H, 4.05; N, 26.26; found C, 48.03; H, 3.99; N, 26.35.

*4.1.1.8.2. 4-(5-Amino-3-(3-(4-fluorophenyl)ureido)-1H-1,2,4-triazol-1-yl)benzenesulfonamide (**21b**)*

Yield (44%); buff powder; m.p. 261–263 °C; IR: 3475, 3363, 3278, 3170 (2NH, $2NH_2$), 1695 (C=O), 1334, 1157 (SO_2); ^{1}H NMR *δ ppm*: 6.87, 6.99 (2s, 2H, -NH_2 of triazole), 7.11- 7.17 (m, 2H, Ar-H), 7.34, 7.45 (2s, 2H, -SO_2NH_2), 7.48-7.54 (m, 2H, Ar-H), 7.63, 7.73 (2d, 2H, Ar-H, *J* = 8.8 Hz), 7.78, 7.90 (2d, 2H, Ar-H, *J* = 8.8 Hz), 7.98, 9.81 (2s, 1H, -NH), 10.22, 10.37 (2s, 1H, -

NH); Anal. Calcd. for $C_{15}H_{14}FN_7O_3S$ (391.38): C, 46.03; H, 3.61; N, 25.05; found C, 45.70; H, 3.54; N, 24.98.

*4.1.1.8.3. 4-(5-Amino-3-(3-(4-chlorophenyl)ureido)-1H-1,2,4-triazol-1-yl)benzenesulfonamide (**21c**)*

Yield (60%); white powder; m.p. 260–262 °C; IR: 3379, 3321, 3286, 3205, 3105 (2NH, $2NH_2$), 1695 (C=O), 1334, 1161 (SO_2); ^{1}H NMR *δ ppm*: 6.88, 7.00 (2s, 2H, -NH_2 of triazole), 7.34- 7.45 (m, 4H, 2H, -SO_2NH_2 and 2H, Ar-H), 7.54, 7.81 (2d, 2H, Ar-H, *J* = 8.8 Hz), 7.63, 7.73 (2d, 2H, Ar-H, *J* = 8.8 Hz), 7.91 (d, 2H, Ar-H, *J* = 8.8 Hz), 7.94, 9.87 (2s, 1H, -NH), 10.13, 10.49 (2s, 1H, -NH); ^{13}C NMR *δ ppm*: 120.51, 120.79, 122.26, 122.48, 123.13, 126.54, 127.29, 127.50, 128.91, 128.97, 129.14, 138.49, 139.82, 140.06, 140.88, 141.98, 151.86, 154.13, 154.54, 155.66, 162.03; Anal. Calcd. for $C_{15}H_{14}ClN_7O_3S$ (407.83): C, 44.18; H, 3.46; N, 24.04; found C, 44.46; H, 3.50; N, 23.94.

*4.1.1.8.4. 4-(5-Amino-3-(3-(p-tolyl)ureido)-1H-1,2,4-triazol-1-yl)benzenesulfonamide (**21d**)*

Yield (53%); buff powder; m.p. 259–261 °C; IR: 3379, 3332, 3294, 3271, 3197 (2NH, $2NH_2$), 1681 (C=O), 1334, 1161 (SO_2); ^{1}H NMR *δ ppm*: 2.25, 2.27 (2s, CH_3), 6.88, 7.00 (2s, 2H, -NH_2 of triazole), 7.10, 7.13 (2d, 2H, Ar-H, *J* = 8.4 Hz), 7.40, 7.65 (2d, 2H, Ar-H, *J* = 8.4 Hz), 7.46, 7.52 (2s, 2H, -SO_2NH_2), 7.74, 7.83 (2d, 2H, Ar-H, *J* = 8.8 Hz), 7.92, 7.97 (2d, 2H, Ar-H, *J* = 8.8 Hz), 7.99, 9.72 (2s, 1H, -NH), 10.00, 10.29 (2s, 1H, -NH); ^{13}C NMR *δ ppm*: 20.83 (CH_3), 20.96 (CH_3), 119.38, 120.66, 122.22, 123.79, 127.30, 127.52, 129.49, 129.68, 131.92, 133.35, 136.27, 136.91, 139.59, 141.94, 143.37, 151.90, 154.13, 154.56, 155.26, 155.97, 157.98, 162.05; HRMS (ESI) for $C_{16}H_{18}O_3N_7{}^{32}S$, calcd 388.11863, found 388.11873 $[M+H]^+$.

*4.1.1.8.5. 4-(5-Amino-3-(3-(4-methoxyphenyl)ureido)-1H-1,2,4-triazol-1-yl)benzenesulfonamide (**21e**)*

Yield (58%); white powder; m.p. 262–264 °C; IR: 3475, 3421, 3344, 3263, 3194 (2NH, $2NH_2$), 1685 (C=O), 1334, 1161 (SO_2); ^{1}H NMR *δ ppm*: 3.73, 3.75 (2s, 3H, OCH_3), 6.88- 7.00 (m, 4H, 2H, Ar-H and 2H, -NH_2 of triazole), 7.42, 7.69 (2d, 2H, Ar-H, *J* = 8.8 Hz), 7.47, 7.53 (2s, 2H, -SO_2NH_2), 7.76, 7.84 (2d, 2H, Ar-H, *J* = 8.4 Hz), 7.93, 7.98 (2d, 2H, Ar-H, *J* = 8.8 Hz), 8.32, 9.70 (2s, 1H, -NH), 10.01, 10.19 (2s, 1H, -NH); ^{13}C NMR *δ ppm*: 55.64 (OCH_3), 114.21, 114.47,

114.92, 115.37, 120.51, 121.16, 122.19, 122.25, 123.76, 127.50, 131.86, 132.41, 139.59, 139.86, 141.90, 143.33, 152.00, 154.13, 155.30, 155.92, 156.12, 157.80; Anal. Calcd. for $C_{16}H_{17}N_7O_4S$ (403.42): C, 47.64; H, 4.25; N, 24.30; found C, 47.45; H, 4.18; N, 24.39.

*4.1.1.8.6. 4-(3-(5-Amino-1-(4-sulfamoylphenyl)-1H-1,2,4-triazol-3-yl)ureido)benzenesulfonamide (**21f**)*

Yield (55%); white powder; m.p. 266–268 °C; IR: 3464, 3379, 3340, 3240 (2NH, $3NH_2$), 1689 (C=O), 1434, 1330, 1161, 1095 (SO_2); ^{1}H NMR δ *ppm*: 6.86, 7.02 (2s, 2H, -NH_2 of triazole), 7.22, 7.34 (2s, 2H, -SO_2NH_2), 7.42-7.45 (m, 3H, 1H, Ar-H and 2H,-SO_2NH_2), 7.63 (d, 1H, Ar-H, *J* = 8.8 Hz), 7.67 (d, 2H, Ar-H, *J* = 8 Hz), 7.72 (d, 2H, Ar-H, *J* = 8 Hz), 7.81 (d, 1H, Ar-H, *J* = 8.8 Hz), 7.90-7.97 (m, 2H, 1H, Ar-H and 1H, -NH), 10.12, 10.71 (2s, 1H, -NH); Anal. Calcd. for $C_{15}H_{16}N_8O_5S_2$ (452.46): C, 39.82; H, 3.56; N, 24.77; found C, 40.20; H, 3.61; N, 24.87.

*4.1.1.8.7. 4-(3-(5-Amino-1-(4-sulfamoylphenyl)-1H-1,2,4-triazol-3-yl)ureido)benzoic acid (**21g**)*

Yield (50%); white powder; m.p. 264–266 °C; IR: 3375, 3348, 3236 (OH, 2NH, $2NH_2$), 1701, 1635 (C=O), 1330, 1161 (SO_2); ^{1}H NMR δ *ppm*: 6.88, 7.01 (2s, 2H, -NH_2 of triazole), 7.34, 7.45 (2s, 2H, -SO_2NH_2), 7.58 (d, 1H, Ar-H, *J* = 8 Hz), 7.63-7.65 (m, 2H, Ar-H), 7.70-7.76 (m, 2H, Ar-H), 7.81 (d, 1H, Ar-H, *J* = 8 Hz), 7.86-7.93 (m, 2H, Ar-H), 7.96, 10.00 (2s, 1H, -NH), 10.13 (s, 1H, -NH), 10.74 (s, 1H, -OH); Anal. Calcd. for $C_{16}H_{15}N_7O_5S$ (417.40): C, 46.04; H, 3.62; N, 23.49; found C, 45.64; H, 3.56; N, 23.39.

4.2 Biological evaluation

4.2.1. CA inhibitory assay

An Applied Photophysics stopped-flow instrument has been used for assaying the CA catalysed CO_2 hydration activity, as reported earlier. [26-28] The inhibition constants were obtained by non-linear least-squares methods using PRISM 3 and the Cheng-Prusoff equation as reported earlier [29], and represent the mean from at least three different determinations. The four tested CA isofoms were recombinant ones obtained in-house as reported earlier [30].

4.2.2. Computational studies

The crystal structure of hCA II (pdb 5LJT) [31], hCA IX (pdb 5FL4) [32] and CA XII (pdb 1JCZ) [33] were prepared using the Protein Preparation Wizard tool implemented in Maestro - Schrödinger suite, assigning bond orders, adding hydrogens, deleting water molecules, and optimizing H-bonding networks [34]. Energy minimization protocol with a root mean square deviation (RMSD) value of 0.30 was applied using an Optimized Potentials for Liquid Simulation (OPLS3e) force field. 3D ligand structures were prepared by Maestro [4a] and evaluated for their ionization states at pH 7.4 ± 0.5 with Epik [4b]. OPLS3e force field in Macromodel [4e] was used for energy minimization for a maximum number of 2500 conjugate gradient iteration and setting a convergence criterion of 0.05 kcal $mol^{-1}Å^{-1}$. The docking grid was centred on the center of mass of the co-crystallized ligands and Glide used with default settings. Ligands were docked with the standard precision mode (SP) of Glide [4f] and the best 5 poses of each molecule retained as output. The best pose for each compound, evaluated in terms of coordination, hydrogen bond interactions and hydrophobic contacts, was refined with Prime [4d] with a VSGB solvation model considering the target flexible within 3Å around the ligand. [35-37] The best poses of **9d** and **21e** to CA IX and CA XII were submitted to a MD simulation using Desmond[38] and the OPL3e force field. Specifically, the system was solvated in an orthorhombic box using TIP4PEW water molecules, extended 15 Å away from any protein atom. It was neutralized adding chlorine and sodium ions. The simulation protocol included a starting relaxation step followed by a final production phase of 100 ns. In particular, the relaxation step comprised the following: (a) a stage of 100 ps at 10 K retaining the harmonic restraints on the solute heavy atoms (force constant of 50.0 kcal mol^{-1} $Å^{-2}$) using the NPT ensemble with Brownian dynamics; (b) a stage of 12 ps at 10 K with harmonic restraints on the solute heavy atoms (force constant of 50.0 kcal mol^{-1} $Å^{-2}$), using the NVT ensemble and Berendsen thermostat; (c) a stage of 12 ps at 10 K and 1 atm, retaining the harmonic restraints and using the NPT ensemble and Berendsen thermostat and barostat; (f) a stage of 12 ps at 300 K and 1 atm, retaining the harmonic restraints and using the NPT ensemble and Berendsen thermostat and barostat; (g) a final 24 ps stage at 300 K and 1 atm without harmonic restraints, using the NPT Berendsen thermostat and barostat. The final production phase of MD was run using a canonical NPT Berendsen ensemble at temperature 300 K. During the MD simulation, a time step of 2 fs was used while constraining the bond lengths of hydrogen atoms with the M-SHAKE algorithm. The atomic coordinates of the system were saved every 100 ps along the MD trajectory. Protein

and ligand RMSD values, ligand torsions evolution and occupancy of intermolecular hydrogen bonds and hydrophobic contacts were computed along the production phase of the MD simulation with the Simulation Interaction Diagram tools implemented in Maestro.

References

[1] R. Kumar, L. Vats, S. Bua, C.T. Supuran, P.K. Sharma, Design and synthesis of novel benzenesulfonamide containing 1,2,3-triazoles as potent human carbonic anhydrase isoforms I, II, IV and IX inhibitors, Eur. J. Med. Chem. 155 (2018) 545-551.

[2] A. Waheed, W.S. Sly, Carbonic anhydrase XII functions in health and disease, Gene, 623 (2017) 33-40.

[3] a) Sentürk, Murat, Ilhami Gülçin, A. Daştan, O. I. Küfrevioğlu, and Claudiu T. Supuran, Carbonic anhydrase inhibitors. Inhibition of human erythrocyte isozymes I and II with a series of antioxidant phenols, Bioorg. Med. Chem. 17 (2009) 3207-3211; b) Innocenti, A., Gülçin, I., Scozzafava, A. and Supuran, C.T. Carbonic anhydrase inhibitors. Antioxidant polyphenols effectively inhibit mammalian isoforms I–XV. Bioorg. Med. Chem. Lett. 20 (2010) 5050-5053; c) Sarikaya, S.B.Ö., Topal, F., Şentürk, M., Gülçin, İ. and Supuran, C.T. In vitro inhibition of α-carbonic anhydrase isozymes by some phenolic compounds. Bioorg. Med. Chem. Lett. 21 (2011) 4259-4262; d) Boztas, M., Cetinkaya, Y., Topal, M., Gulcin, I., Menzek, A., Sahin, E., Tanc, M. and Supuran, C.T., Synthesis and carbonic anhydrase isoenzymes I, II, IX, and XII inhibitory effects of dimethoxybromophenol derivatives incorporating cyclopropane moieties J. Med. Chem. 58 (2014) 640-650.

[4] C.T. Supuran, V. Alterio, A. Di Fiore, K. D'Ambrosio, F. Carta, S.M. Monti, G. De Simone, Inhibition of carbonic anhydrase IX targets primary tumors, metastases, and cancer stem cells: three for the price of one, Medicinal research reviews, 38 (2018) 1799-1836.

[5] M.Y. Mboge, R. McKenna, S.C. Frost, Advances in anti-cancer drug development targeting carbonic anhydrase IX and XII, Topics in anti-cancer research, 5 (2015) 3.

[6] V. Alterio, A. Di Fiore, K. D'Ambrosio, C.T. Supuran, G. De Simone, Multiple Binding Modes of Inhibitors to Carbonic Anhydrases: How to Design Specific Drugs Targeting 15 Different Isoforms? Chem. Rev. 112 (2012) 4421-4468.

[7] C.T. Supuran, How many carbonic anhydrase inhibition mechanisms exist? J. Enzyme Inhib. Med. Chem. 31 (2016) 345-360.

[8] M.F. Abo-Ashour, W.M. Eldehna, A. Nocentini, H.S. Ibrahim, S. Bua, H.A. Abdel-Aziz, S.M. Abou-Seri, C.T. Supuran, Novel synthesized SLC-0111 thiazole and thiadiazole analogues: Determination of their carbonic anhydrase inhibitory activity and molecular modeling studies, Bioorg. Chem., 87 (2019) 794-802.

[9] V. Sharma, R. Kumar, S. Bua, C.T. Supuran, P.K. Sharma, Synthesis of novel benzenesulfonamide bearing 1,2,3-triazole linked hydroxy-trifluoromethylpyrazolines and hydrazones as selective carbonic anhydrase isoforms IX and XII inhibitors, Bioorg. Chem. 85 (2019) 198-208.

[10] M.G. El-Gazzar, N.H. Nafie, A. Nocentini, M.M. Ghorab, H.I. Heiba, C.T. Supuran, Carbonic anhydrase inhibition with a series of novel benzenesulfonamide-triazole conjugates, J. Enzym. Inhib. Med. Chem. 33 (2018) 1565-1574.

[11] F. Carta, M. Ferraroni, A. Scozzafava, C.T. Supuran, Fluorescent sulfonamide carbonic anhydrase inhibitors incorporating 1, 2, 3-triazole moieties: kinetic and X-ray crystallographic studies, Bioorg. Med. Chem. 24 (2016) 104-112.

[12] M. Fares, R.A. Eladwy, A. Nocentini, S.R.A. El Hadi, H.A. Ghabbour, A. Abdel-Megeed, W.M. Eldehna, H.A. Abdel-Aziz, C.T. Supuran, Synthesis of bulky-tailed sulfonamides incorporating pyrido[2,3-d][1,2,4]triazolo[4,3-a]pyrimidin-1(5*H*)-yl) moieties and evaluation of their carbonic anhydrases I, II, IV and IX inhibitory effects, Bioorg. Med. Chem. 25 (2017) 2210-2217.

[13] W.M. Eldehna, M.F. Abo-Ashour, A. Nocentini, R.S. El-Haggar, S. Bua, A. Bonardi, S.T. Al-Rashood, G.S. Hassan, P. Gratteri, H.A. Abdel-Aziz, Enhancement of the tail hydrophobic interactions within the carbonic anhydrase IX active site via structural extension: Design and synthesis of novel *N*-substituted isatins-SLC-0111 hybrids as carbonic anhydrase inhibitors and antitumor agents, Eur. J. Med. Chem., 162 (2019) 147-160.

[14] W.M. Eldehna, M.F. Abo-Ashour, E. Berrino, D. Vullo, H.A. Ghabbour, S.T. Al-Rashood, G.S. Hassan, H.M. Alkahtani, A.A. Almehizia, A. Alharbi, SLC-0111 enaminone analogues, 3/4-(3-aryl-3-oxopropenyl) aminobenzenesulfonamides, as novel selective subnanomolar inhibitors of the tumor-associated carbonic anhydrase isoform IX, Bioorg. Chem., 83 (2019) 549-558.

[15] W.M. Eldehna, M.A. Abdelrahman, A. Nocentini, S. Bua, S. T. Al-Rashood, G. S. Hassan, A. Bonardi, A.A. Almehizia, H.M. Alkahtani, A. Alharbi, P. Gratteri, C.T. Supuran, Synthesis,

biological evaluation and *in silico* studies with 4-benzylidene-2-phenyl-5(4*H*)-imidazolone-based benzenesulfonamides as novel selective carbonic anhydrase IX inhibitors endowed with anticancer activity, Bioorg. Med. Chem. 90 (2019) 2210-2217.

[16] M.A. Abdelrahman, W.M. Eldehna, A. Nocentini, S. Bua, S. T. Al-Rashood, G. S. Hassan, A. Bonardi, A.A. Almehizia, H.M. Alkahtani, A. Alharbi, P. Gratteri, C.T. Supuran, Novel Diamide-Based Benzenesulfonamides as Selective Carbonic Anhydrase IX Inhibitors Endowed with Antitumor Activity: Synthesis, Biological Evaluation and In Silico Insights, Int. J. Mol. Sci. 20 (2019) 2484.

[17] V.A. Pivazyan, E.A. Ghazaryan, R.S. Shainova, R.A. Tamazyan, A.G. Ayvazyan, A.P. Yengoyan, Synthesis and Growth Stimulant Properties of 2-Acetyl-3, 7-dimethyl-5H-thiazolo [3, 2-a] pyrimidin-5-one Derivatives, J. Chem. (2017) Article ID 8180913.

[18] M. Fares, S.M. Abou-Seri, H.A. Abdel-Aziz, S.E.-S. Abbas, M.M. Youssef, R.A. Eladwy, Synthesis and antitumor activity of pyrido[2,3-d]pyrimidine and pyrido[2,3-d][1,2,4]triazolo[4, 3-a]pyrimidine derivatives that induce apoptosis through G1 cell-cycle arrest, Eur. J. Med. Chem. 83 (2014) 155-166.

[19] M.A. Said, W.M. Eldehna, H.A. Ghabbour, M.M. Kabil, N.S. Al-shakliah, H.A. Abdel-Aziz, Solvent-Free Ring Cleavage Hydrazinolysis of Certain Biginelli Pyrimidines, J. Chem. (2018) Article ID 6354742.

[20] C.-H. Chien, M.-k. Leung, J.-K. Su, G.-H. Li, Y.-H. Liu, Y. Wang, Substituent effects on pyrid-2-yl ureas toward intramolecular hydrogen bonding and cytosine complexation, J. Org. Chem. 69 (2004) 1866-1871.

[21] L. Fischer, G.J.O. Guichard, Folding and self-assembly of aromatic and aliphatic urea oligomers: Towards connecting structure and function, Org. Biomol. Chem. 8 (2010) 3101-3117.

[22] A. Tarai, J. Baruah, Conformation and Visual Distinction between Urea and Thiourea Derivatives by an Acetate Ion and a Hexafluorosilicate Cocrystal of the Urea Derivative in the Detection of Water in Dimethylsulfoxide, ACS Omega 2 (2017) 6991-7001.

[23] R.G. Khalifah, The carbon dioxide hydration activity of carbonic anhydrase I. Stop-flow kinetic studies on the native human isoenzymes B and C, J. Biol. Chem. 246 (1971) 2561-2573.

[24] A. Nocentini, C.T. Supuran, Advances in the structural annotation of human carbonic anhydrases and impact on future drug discovery, Expert Opin. Drug Discov. (2019) 1-23.

[25] S.-X. Gu, S.-Q. Yang, Q.-Q. He, X.-D. Ma, F.-E. Chen, H.-F. Dai, E. De Clercq, J. Balzarini, C. Pannecouque, Design, synthesis and biological evaluation of cycloalkyl arylpyrimidines (CAPYs) as HIV-1 NNRTIs, m. chemistry, Bioorg. Med. Chem. 19 (2011) 7093-7099.

[26] A. Nocentini, M. Ceruso, S. Bua, C.L. Lomelino, J.T. Andring, R. McKenna, C. Lanzi, S. Sgambellone, R. Pecori, R. Matucci, Discovery of β-Adrenergic Receptors Blocker–Carbonic Anhydrase Inhibitor Hybrids for Multitargeted Antiglaucoma Therapy, J. Med. Chem. 61 (2018) 5380-5394.

[27] Y.E. Heravi, S. Bua, A. Nocentini, S. Del Prete, A.A. Saboury, H. Sereshti, C. Capasso, P. Gratteri, C.T. Supuran, Inhibition of Malassezia globosa carbonic anhydrase with phenols, Bioorg. Med. Chem. 25 (2017) 2577-2582.

[28] A. Nocentini, D. Moi, G. Balboni, V. Onnis, C.T. Supuran, Discovery of thiazolin-4-one-based aromatic sulfamates as a new class of carbonic anhydrase isoforms I, II, IV, and IX inhibitors, Bioorg. Chem. 77 (2018) 293-299.

[29] W.M. Eldehna, A. Nocentini, A. Bonardi, S. Bua, H.S. Ibrahim, M.M. Elaasser, V. Kryštof, R. Jorda, P. Gratteri, S.M. Abou-Seri, C.T. Supuran, 3-Hydrazinoisatin-based benzenesulfonamides as novel carbonic anhydrase inhibitors endowed with anticancer activity: Synthesis, *in vitro* biological evaluation and *in silico* insights, Eur. J. Med. Chem. 2019, Accepted manuscript.

[30] a) W.M. Eldehna, A. Nocentini, S.T. Al-Rashood, G.S. Hassan, H.M. Alkahtani, A.A. Almehizia, A.M. Reda, H.A. Abdel-Aziz, C.T.J.B.c. Supuran, Tumor-associated carbonic anhydrase isoform IX and XII inhibitory properties of certain isatin-bearing sulfonamides endowed with in vitro antitumor activity towards colon cancer, 81 (2018) 425-432; b) M.M. Al-Sanea, A. Elkamhawy, S. Paik, S. Bua, S.H. Lee, M.A. Abdelgawad, E.J. Roh, W.M. Eldehna, C.T. Supuran, Synthesis and biological evaluation of novel 3-(quinolin-4-ylamino)benzenesulfonamides as carbonic anhydrase isoforms I and II inhibitors, J. Enzyme Inhib. Med. Chem. 2019, 34, 1457-1464.

[31] a) A. Nocentini, M. Ferraroni, F. Carta, M. Ceruso, P. Gratteri, C. Lanzi, E. Masini, C.T. Supuran, Benzenesulfonamides incorporating flexible triazole moieties are highly effective carbonic anhydrase inhibitors: synthesis and kinetic, crystallographic, computational, and intraocular pressure lowering investigations, J. Med. Chem. 59 (2016) 10692-10704. b) C.T.

Supuran, M.A. Ilies, A. Scozzafava, Carbonic anhydrase inhibitors. Part 29. Interaction of isozymes I, II and IV with benzolamide-like derivatives. Eur. J. Med. Chem. 1998, 33, 739-752

[32] J. Leitans, A. Kazaks, A. Balode, J. Ivanova, R. Zalubovskis, C.T. Supuran, K. Tars, Efficient expression and crystallization system of cancer-associated carbonic anhydrase isoform IX, J. Med. Chem. 58 (2015) 9004-9009.

[33] D.A. Whittington, A. Waheed, B. Ulmasov, G.N. Shah, J.H. Grubb, W.S. Sly, D.W. Christianson, Crystal structure of the dimeric extracellular domain of human carbonic anhydrase XII, a bitopic membrane protein overexpressed in certain cancer tumor cells, Proc. Natl. Acad. Sci. U. S. A. 98 (2001) 9545-9550.

[34] S. Kalinin, A. Nocentini, A. Kovalenko, V. Sharoyko, A. Bonardi, A. Angeli, P. Gratteri, T.B. Tennikova, C.T. Supuran, M. Krasavin, From random to rational: A discovery approach to selective subnanomolar inhibitors of human carbonic anhydrase IV based on the Castagnoli-Cushman multicomponent reaction, Eur. J. Med. Chem. (2019) 111642.

[35] A. Nocentini, P. Gratteri, C.T. Supuran, Phosphorus versus Sulfur: Discovery of Benzenephosphonamidates as Versatile Sulfonamide-Mimic Chemotypes Acting as Carbonic Anhydrase Inhibitors, CHEM-EUR J. 25 (2019) 1188-1192.

[36] A. Nocentini, A. Bonardi, P. Gratteri, B. Cerra, A. Gioiello, C.T. Supuran, Steroids interfere with human carbonic anhydrase activity by using alternative binding mechanisms, J. Enzyme Inhib. Med. Chem. 33 (2018) 1453-1459.

[37] Nocentini A, Carta F, Tanc M, Selleri S, Supuran CT, Bazzicalupi C, Gratteri P.Deciphering the Mechanism of Human Carbonic Anhydrases Inhibition with Sulfocoumarins: Computational and Experimental Studies. Chemistry 24 (2018) 7840-7844.

[38] Schrödinger Release 2019-2: Desmond Molecular Dynamics System, D. E. Shaw Research, New York, NY, 2019, v.5.7.

Highlights

- New series of triazolopyrimidine/triazole-based benzenesulfonamides were synthesized.

- Inhibitory activities of all derivatives were evaluated toward hCA I, II, IX and XII isoforms.

- hCA IX and XII were efficiently inhibited with K_Is range of 3.3-85 nM and 4.4-105 nM.

- **9d** and **21e** were found to be the most selective *h*CA IX inhibitors over *h*CA I and *h*CA II.

- Molecular modeling was done to acquire insights for the binding interactions and affinities.

Declaration of Interest Statement

Conflicts of Interest: The authors have declared no conflict of interest.